CMS-TOP-16-020

arXiv:1712.02825v2 [hep-ex] 5 Mar 2018

Measurement of the associated production of a single top quark and a Z boson in pp collisions at $\sqrt{s} = 13\,\text{TeV}$

The CMS Collaboration[*]

Abstract

A measurement is presented of the associated production of a single top quark and a Z boson. The study uses data from proton-proton collisions at $\sqrt{s} = 13\,\text{TeV}$ recorded by the CMS experiment, corresponding to an integrated luminosity of $35.9\,\text{fb}^{-1}$. Using final states with three leptons (electrons or muons), the tZq production cross section is measured to be $\sigma(\text{pp} \to \text{tZq} \to \text{Wb}\ell^+\ell^-\text{q}) = 123^{+33}_{-31}\,(\text{stat})^{+29}_{-23}\,(\text{syst})\,\text{fb}$, where ℓ stands for electrons, muons, or τ leptons, with observed and expected significances of 3.7 and 3.1 standard deviations, respectively.

*See Appendix B for the list of collaboration members

1 Introduction

At the CERN LHC, single top quark production proceeds through three electroweak interaction processes: t-channel, s-channel, and associated tW production. Cross sections for single top quark production have been reported by the CDF and D0 Collaborations [1, 2], as well as by the ATLAS [3–7] and CMS [8–11] Collaborations.

The high centre-of-mass proton-proton (pp) collision energy of 13 TeV at the LHC, together with large integrated luminosities, allows the study of processes with very small cross sections that were not accessible at lower energies. One example of such a process is the rare associated production of a single top quark with a Z boson. This production mechanism, leading to a final state with a top quark, a Z boson, and an additional quark, can probe the standard model (SM) in a unique way. The main leading-order (LO) diagrams that contribute to this final state are shown in Fig. 1. Although generically denoted in this Letter by tZq, this process also includes a small contribution from non-resonant lepton pairs, as shown in the lower right-hand diagram in Fig. 1. The process is sensitive to top quark couplings to the Z boson, as illustrated in the middle right-hand diagram in Fig. 1, and also to the triple gauge-boson coupling WWZ, as illustrated in the lower left-hand diagram in Fig. 1.
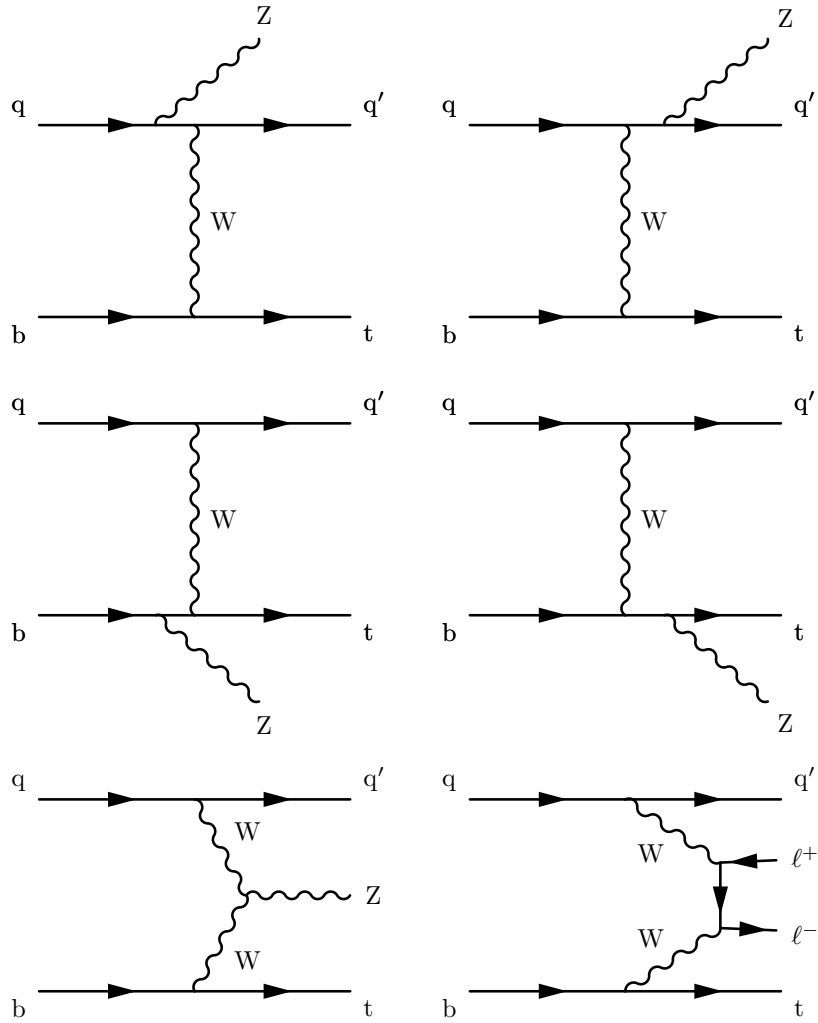

Figure 1: Leading-order tZq production diagrams. The lower right-hand diagram represents the non-resonant contribution to the tZq process.

The top quark couplings to the Z boson and the triple gauge-boson couplings are sensitive to new physical phenomena. In particular, measurements of tZq production are sensitive to processes beyond the SM that have similar experimental signatures, such as flavour-changing neutral currents (FCNC) involving the direct coupling of the top quark to a Z boson and an up or charm quark, at the top quark production or decay [12, 13]. Within the SM, FCNC processes are forbidden at LO and suppressed at higher orders [14]. Deviations from the expected SM tZq production could therefore be indicative of beyond-SM FCNC processes.

The next-to-leading-order (NLO) cross section for $\text{tZq} \to \text{Wb}\ell^+\ell^-\text{q}$, considering only the leptonic decays of Z bosons (to electrons, muons, or τ leptons, generically denoted by ℓ), is calculated for pp collisions at a centre-of-mass energy of 13 TeV, using the Monte Carlo (MC) generator MADGRAPH5_aMC@NLO 2.2.2 [15]. The calculation, which includes lepton pairs from off-shell Z bosons with invariant mass $m_{\ell^+\ell^-} > 30$ GeV, uses the NNPDF 3.0 set of parton distribution functions (PDFs) [16] in the five-flavour scheme. The result is $\sigma^{\text{SM}}(\text{t}\ell^+\ell^-\text{q}) = 94.2^{+1.9}_{-1.8}$ (scale) ± 2.5 (PDF) fb, with the "scale" and "PDF" uncertainties estimated, respectively, by changing the quantum chromodynamics (QCD) renormalization and factorization scales by factors of 0.5 and 2, and by using the 68% confidence level (CL) uncertainty on the NNPDF3.0 PDF set. This cross section is used as the reference in this analysis. Another calculation, including all Z boson decays, gives a compatible cross section when the branching fraction to charged leptons is taken into account [17]. Previous searches for tZq production at 8 TeV by the CMS Collaboration [18] reported a signal with a significance of 2.4 standard deviations. The ATLAS Collaboration recently reported a measurement of the tZq production cross section at 13 TeV [19] with a significance of 4.2 standard deviations.

This Letter presents a search for tZq production in pp collisions at $\sqrt{s} = 13$ TeV, using data collected in 2016 by CMS, corresponding to an integrated luminosity of 35.9 fb^{-1}. The signature for tZq production consists of a single top quark produced in the t channel, a Z boson, and an additional ("recoiling") jet emitted at pseudorapidity $|\eta| < 4.5$. The analysis uses events where the Z boson decays to e^+e^- or $\mu^+\mu^-$, while the W boson, produced in the decay of the top quark, decays to a neutrino and an electron or a muon, resulting in four possible final-state leptonic combinations: eee, eeμ, e$\mu\mu$, and $\mu\mu\mu$. There will also be a small contribution from τ leptons decaying into electrons or muons. The final result reflects an extrapolation to include all decay modes involving τ leptons. The measurement is based on a multivariate analysis, where boosted decision trees (BDTs) [20] are used to enhance the signal-to-background separation. Several control regions are defined to better constrain the backgrounds, each containing different contributions from signal and background processes.

2 The CMS detector

The central feature of the CMS apparatus is a superconducting solenoid of 6 m internal diameter, providing a magnetic field of 3.8 T. Within the solenoid volume are a silicon pixel and strip tracker, a lead tungstate crystal electromagnetic calorimeter (ECAL), and a brass and scintillator hadron calorimeter (HCAL), each composed of a barrel and two endcap sections. Forward calorimeters extend the pseudorapidity coverage provided by the barrel and endcap detectors. Muons are measured in gas-ionization detectors embedded in the steel flux-return yoke outside the solenoid. The electron momentum is evaluated by combining the energy measurement in the ECAL with the momentum measurement in the tracker. The momentum resolution for electrons with transverse momentum, p_{T}, around 45 GeV from $Z \to$ ee decays ranges from 1.7% for nonshowering electrons in the barrel region to 4.5% for showering electrons in the endcaps [21]. Muons are measured in the range $|\eta| < 2.4$, with detection planes made using

three technologies: drift tubes, cathode strip chambers, and resistive plate chambers. Matching muons to tracks measured in the silicon tracker results in a relative transverse momentum resolution for muons with $20 < p_T < 100$ GeV of 1.3–2.0% in the barrel and better than 6% in the endcaps [22]. A more detailed description of the CMS detector, together with a definition of the coordinate system used and the relevant kinematic variables, can be found in Ref. [23].

Events of interest are selected using a two-tiered trigger system [24]. The first level, composed of custom hardware processors, uses information from the calorimeters and muon detectors to select events at a rate of around 100 kHz within a time interval of less than 4 μs. The second level, known as the high-level trigger, consists of a farm of processors running a version of the full event reconstruction software optimised for fast processing, and reduces the event rate to less than 1 kHz before data storage.

3 Online selection, reconstruction, and identification

The data are selected online using triggers that rely on the presence of either one, two, or three high-p_T leptons. The lowest p_T thresholds of the three-lepton triggers are 16, 12, and 8 GeV for electrons, and 12, 10, and 5 GeV for muons; the corresponding values for the dilepton triggers are 23 and 12 GeV for electrons, and 17 and 8 GeV for muons. Triggers requiring the presence of at least one electron and at least one muon are also used. For the baseline offline selection, a trigger efficiency of nearly 100% is achieved by including single-lepton triggers with thresholds of 32 and 24 GeV for electrons and muons, respectively, in addition to the two- and three-lepton triggers.

The events are reconstructed using the particle-flow (PF) algorithm [25], which reconstructs and identifies each individual particle with an optimised combination of information from the various elements of the CMS detector. The energy of the photons is directly obtained from the ECAL measurement, corrected for zero-suppression effects, while that of the electrons is determined from a combination of the electron momentum at the primary interaction vertex as determined by the tracker, the energy of the corresponding ECAL cluster, and the total energy of all bremsstrahlung photons spatially compatible with originating from the electron track. The energy of the muons is obtained from the curvature of the corresponding track. The energy of charged hadrons is determined from a combination of their momentum, measured in the tracker, and the matching ECAL and HCAL energy deposits, corrected for zero-suppression effects and for the response function of the calorimeters to hadronic showers. Finally, the energy of neutral hadrons is obtained from the corresponding ECAL and HCAL corrected energy deposits. For each event, jets are clustered from the PF candidates using the anti-k_T algorithm [26, 27], with a distance parameter of 0.4. The reconstructed vertex with the largest value of summed physics-object p_T^2 is taken to be the primary pp interaction vertex. The physics objects are the jets, clustered with the tracks assigned to the vertex as inputs, and the associated missing transverse momentum, taken as the negative vector sum of the p_T of those jets. All charged particles considered in this analysis are required to be compatible with originating from the primary interaction vertex.

The event selection relies on the concept of relative lepton isolation, reflected in the variable I_{rel}, computed as the scalar sum of the p_T of all particles in a cone of radius $\Delta R = \sqrt{(\Delta \eta)^2 + (\Delta \phi)^2}$ around the lepton (where ϕ is the azimuth), excluding the lepton, and divided by the lepton p_T. The sum is then corrected for the neutral particles produced in extra pp interactions within the same or neighbouring LHC bunch crossings, referred to as pileup (PU) collisions. For electrons, ΔR is set to 0.3, and the expected PU within the isolation cone is estimated from

the median energy density per area of PU contamination. Muon I_{rel} uses $\Delta R = 0.4$, and is corrected for the average neutral PU energy inside the isolation cone, which has been measured in multijet events to be one half of the energy coming from charged hadrons not associated with the primary vertex. Electrons and muons are considered isolated if I_{rel} is smaller than 0.06 and 0.15, respectively.

The data with prompt leptons are contaminated by genuine leptons from hadron decays (usually referred to as "nonprompt leptons") and by hadrons or jets misidentified as leptons (usually referred to as "fake leptons"). In addition, nonprompt isolated electrons can arise from the conversion of photons. For simplicity of notation, and given that these background sources are evaluated with similar methods, based on control samples in data, all such sources are referred to as "not-prompt" leptons, or simply "NPL", in this Letter. Data samples for evaluating the NPL background are built using objects reconstructed similarly to the prompt leptons, with two important differences. First, while the prompt and not-prompt leptons are identified using the same variables [21, 22], less stringent criteria are applied to the NPL sample. Second, leptons are considered not-prompt only if they are not isolated, requiring not-prompt electrons or muons to have $I_{rel} > 0.17$ or > 0.25, respectively. In addition, not-prompt electrons are required to have $I_{rel} < 1$, removing a large fraction of photons with $I_{rel} \approx 1$ and Z+jets events containing a low-p_T jet misidentified as a high I_{rel} electron. Tight criteria to reject photon conversions [21] are required for both prompt and not-prompt electrons.

The jet momentum is determined from the vectorial sum of all particle momenta in the jet, and is found in simulation studies to be within 5 to 10% of the true momentum over the whole p_T spectrum and detector acceptance. Jet energy corrections are obtained from simulation studies and confirmed with in situ measurements through the balance in dijet, multijet, photon+jet, and leptonic Z+jet events [28]. In the central region, the jet energy resolution is approximately 15% at 10 GeV, 8% at 100 GeV, and 4% at 1 TeV. Jets reconstructed at angular distances $\Delta R < 0.4$ from the selected leptons are not considered for further analysis. As the region $2.7 < |\eta| < 3.0$ is particularly affected by noise, events with jets of $p_T < 50$ GeV in that region are rejected.

Jets that originate from the hadronization of a b quark are identified (tagged) using the combined secondary vertex (CSVv2) algorithm [29, 30], which combines various track-based variables with secondary-vertex variables to construct a discriminating observable in the region $|\eta| < 2.4$. At the chosen operating point, the CSVv2 algorithm has an efficiency of about 83% to correctly tag b jets and a probability of 10% for mistagging gluons and light quarks, as estimated from simulation studies of multijet events.

The missing transverse momentum vector $\vec{p}_T^{\,miss}$ is defined as the projection onto the plane perpendicular to the beam axis of the negative vector sum of the momenta of all reconstructed PF objects in an event. Its magnitude is denoted by p_T^{miss}. The transverse mass of the W boson is defined as $m_T^W = \sqrt{2p_T p_T^{miss}[1 - \cos(\Delta\phi)]}$, where p_T is the transverse momentum of the lepton produced in the W boson decay, and $\Delta\phi$ is the difference in azimuth between the direction of the lepton and the direction of $\vec{p}_T^{\,miss}$.

4   Simulated events

Monte Carlo simulated events are used extensively in this measurement to evaluate the detector resolution, the efficiencies and acceptance, and to estimate the contributions from background processes that have topologies similar to the trilepton tZq final state.

The tZq signal samples are generated at NLO precision using the MADGRAPH5_aMC@NLO

2.2.2 package [15]. The two main background processes, WZ+jets and top quark pair production in association with vector bosons ($t\bar{t}Z$ and $t\bar{t}W$), are also simulated with the same event generator, with up to one additional hadronic jet at NLO. Other minor backgrounds are ZZ and $t\bar{t}H$ production, for which we use the NLO generators MADGRAPH5_aMC@NLO and POWHEG v2.0 [31–36], respectively, and tWZ production, generated at LO accuracy using MAD-GRAPH5_aMC@NLO. The PDF set NNPDF 3.0 is used in all generators. The simulated samples are interfaced to PYTHIA 8.205 [37] with the CUETP8M1 tune [38] for the parton shower and hadronization. The detector response is simulated using the GEANT4 package [39].

The events are simulated in final states that include decays to electrons, muons, and τ leptons. A top quark mass of 172.5 GeV is assumed. Multiple minimum-bias events generated with PYTHIA are added to each simulated event to mimic the presence of PU, with weights that reproduce the measured distribution of the number of PU vertices.

The event samples are normalized to their expected cross sections, obtained from NLO calculations for all processes, except for tWZ, which is estimated at LO accuracy.

Correction factors that depend on the p_T and η of the jets and leptons are applied to the samples, so that the resolutions, energy scales, and efficiencies measured in data are well reproduced by the simulation. The corrections include an extra smearing of the jet energy, which has a better resolution in the simulation than found in data, and scale factors that account for different efficiencies in lepton identification and reconstruction. The shape of the distribution in the CSVv2 discriminant is one of the variables used in the multivariate analysis to extract the signal. The simulated shape has been corrected [29, 30] to assure that the b tagging efficiency and purity variables reproduce those found in data.

One of the most abundant background sources in the three-lepton final state arises from events with at least one NPL. Unlike all other backgrounds, which are modelled by MC simulation, the samples used to estimate the NPL background contribution are obtained from the data, as described in Section 6.2.

5 Event selection: signal and background control regions

The event selection makes use of tZq event candidates where $t \rightarrow Wb$, $W \rightarrow l\nu$, and $Z \rightarrow l'^{+}l'^{-}$,

$$tZq \rightarrow (t \rightarrow bl\nu)\,(Z \rightarrow l'^{+}l'^{-})q,$$

where l and l' are either electrons or muons, coming from the W or Z boson decay, respectively, as opposed to generic leptons (including τ leptons), which have been denoted by ℓ. As stated in Section 1, l includes a small contribution from $W \rightarrow \tau\nu$ decays, with the subsequent decay of the τ into electrons or muons. The final result will be given for all decay modes to a generic lepton, ℓ. In single top quark production, the associated recoil jet usually follows the direction of the incoming proton, so it is detected in the very forward regions of the detector. For this reason, we select jets in the extended pseudorapidity range $|\eta| < 4.5$. Given the tracker acceptance, b-tagged jets are confined to the $|\eta| < 2.4$ range. All jets, both tagged and untagged, are required to have $p_T > 30$ GeV.

The baseline selection for the analysis consists in exactly three leptons, two of which have the same flavour, are oppositely charged, and have an invariant mass compatible with the Z boson mass within 15 GeV. Electrons and muons are required to have $p_T > 25$ GeV, and to be measured within $|\eta| < 2.5$ and 2.4, respectively. To reduce backgrounds from four or more leptons in the final state, e.g. from ZZ, $t\bar{t}Z$, and $t\bar{t}H$, events containing additional leptons with $p_T > 10$ GeV and passing looser identification criteria are removed from the analysis.

Several other SM processes, some of which have much larger cross sections than expected for tZq, contain three reconstructed leptons in the final state. Out of these, the most important are the WZ+jets, the $t\bar{t}Z$, and those contributing to the NPL background. For the first two, the three-lepton topology is identical to tZq: two oppositely charged leptons of same flavour decaying from the Z boson, and a third high-p_T, isolated lepton. The $t\bar{t}Z$ production for the four-lepton final state has a smaller cross section than that for the three-lepton final state, and is also suppressed by the already mentioned veto on events with four or more leptons. Although the misidentification rate per lepton, especially for muons, is small, the cross sections of the processes producing the NPL background (dominated by Drell–Yan production in association with jets, DY+jets, and $t\bar{t}$ production) are orders of magnitude larger than the expected tZq cross section, making NPL one of the most important backgrounds to the three-lepton final state.

For the tZq final state, two jets are expected, one of which arises from a b quark. In the $t\bar{t}Z$ three-lepton final state, two b jets are expected. However, given the inefficiencies of the b tagging algorithm, one of the two b jets may be untagged, leading to a final state identical to the signal. Likewise, one of the b jets produced by gluon splitting in the WZ+jets final states may be tagged, or, most frequently, light-flavour jets from WZ+jets production can be mistagged as b jets, again resulting in a topology identical to the signal.

To reduce the impact of the background-related uncertainties on the measurement of the tZq yield, we proceed as follows. The baseline three-lepton selection is subdivided into three regions of interest, one enriched in tZq events, another selected to contain mostly $t\bar{t}Z$ events, and a third containing mostly WZ+jets and NPL background events. The final analysis performs a simultaneous fit to these three regions, so that the signal cross section is determined and the normalizations of the main backgrounds are better constrained.

The three regions are defined according to their jet and b-tagged jet multiplicities, as follows:

1. 1bjet (signal region): defined to select events from tZq production with one b jet and one recoiling jet. Events with a third jet are also included, to cover cases where an additional jet is produced by radiation.

2. 2bjets control region ($t\bar{t}Z$ enriched): defined by requiring at least two jets, with at least two of them b tagged, enhancing thereby the yield in $t\bar{t}Z$ events.

3. 0bjet control region (WZ+jets enriched): defined by at least one jet, but no b-tagged jets, selected as most likely originating from a WZ process. Since the majority of DY+jets events also do not contain b jets, this region is also rich in NPL background events.

6   Shape-based analysis

The tZq cross section is extracted from a binned maximum-likelihood fit to the distributions in the BDT discriminators (to be defined later) in the 2bjets and 1bjet regions, and to the m_T^W distribution in the 0bjet region. Normalized distributions (templates) are constructed using these variables in their respective regions, for each of the four final states (eee, eeμ, e$\mu\mu$, and $\mu\mu\mu$), adding up to 12 distributions that are simultaneously fitted.

6.1   Input normalization of the SM predictions

The input (pre-fit) normalizations of the simulated backgrounds reflect their corresponding theoretical cross sections. The contributions from WZ+b, WZ+c, and WZ+light-flavour jets in

the WZ+jets MC events are separated using generator-level information, and considered as independent backgrounds in all steps of the analysis. This provides a better modelling of the heavy-flavour content of the WZ+jets sample, and avoids relying on the flavour content of the MC simulation.

6.2   The NPL background

The templates for the NPL background are based on data. The origin of not-prompt leptons depends on the lepton flavour. For muons, the dominant source is the semileptonic decay of heavy-flavour hadrons. In the case of electrons, the dominant sources are photon conversions and light hadrons that are misreconstructed as electrons. The not-prompt electrons and muons are therefore treated as separate background sources.

The background events containing not-prompt leptons originate from, in order of importance, DY+jets processes, $t\bar{t}$ events containing two leptons, and WW and tW processes. Each of these background sources contain two prompt and one not-prompt leptons. Given the low probability that an NPL is identified as a prompt lepton, the contribution from events with more than one NPL is negligible. Not-prompt electron (muon) templates are obtained from events containing exactly one not-prompt electron (muon), identified as described in Section 3, and two prompt leptons (either electrons or muons). In the NPL sample, the not-prompt leptons can be associated either with the top quark or with the Z boson candidates.

The samples used to obtain the NPL background templates are quite copious, typically having two orders of magnitude more events than the signal sample obtained with the baseline selection. While the shapes of the distributions used in the multivariate analysis are provided by templates, their normalizations are determined through a two-step procedure. In the first step, the m_T^W distribution in the 0bjet control region provides the normalization of all NPL components, independently in the four channels. This fixes the relative NPL normalization of the templates in the four channels. In a subsequent step, the not-prompt electron and muon yields are treated as free and independent parameters, in a simultaneous fit of the 0bjet/1bjet/2bjets regions. This second step represents the final fit used to provide the results reported in this Letter.

The use of the 0bjet region to provide the relative NPL yields in the four channels is justified by the dominance of the DY process as source of NPL background events in all three b tagging regions. To check the validity of the procedure, an independent analysis is performed where the weight of the DY background relative to $t\bar{t}$ production is suppressed by means of mild requirements on p_T^{miss} and m_T^W. In this cross-check analysis, the relative normalizations of the not-prompt electron and muon backgrounds are left free in the four channels, and the results are obtained in a single common fit. This alternative procedure gives similar final results.

6.3   Multivariate analysis

The signal extraction relies on a simultaneous fit to the data in the three regions defined in Section 5, to better constrain the backgrounds in the signal region.

Two multivariate discriminators, based on observables from the 1bjet and 2bjets regions, are used to enhance the separation between signal and background processes. The discriminators are based on the BDT algorithm [20] implemented in the toolkit for multivariate analysis TMVA [40]. The BDT is trained using the simulated samples described in Section 4.

Several observables serve as input variables for the BDT. These include the reconstructed top quark mass and distributions of variables reflecting the kinematics and the angles of the recoiling jet, of the top quark, and of the Z boson, as well as those of their decay products. Once the

two oppositely charged leptons of same flavour are identified as Z boson decay products, the additional lepton is assumed to arise from the decay $W \rightarrow l\nu$. The longitudinal component of the neutrino momentum is calculated using the W mass constraint for the $l + \nu$ system, and assuming the event p_T^{miss} to be equal to the transverse momentum of the neutrino. The reconstructed W boson candidate is then associated to a b-jet candidate for the t $\rightarrow$ Wb hypothesis. The b-jet candidate is the tagged jet. If two solutions are found for the longitudinal component of the neutrino momentum, or if more than one jet is tagged (in the 2bjets region), the solution giving the Wb candidate invariant mass closest to that of the top quark is taken. The remaining jet with the largest p_T is taken as the recoiling jet. The information related to b tagging is also used through the distributions of the CSVv2 discriminant [29, 30] and the b-tagged jet multiplicity.

Variables computed using the matrix element method (MEM) [41] are also included in the multivariate analysis. A weight $w_{i,\alpha}$ is computed for each event i and hypothesis α (where α is either signal, t$\bar{t}$Z, or WZ+jets) as

$$w_{i,\alpha}(\Phi') = \frac{1}{\sigma_\alpha} \int d\Phi_\alpha \, \delta^4\left(p_1^\mu + p_2^\mu - \sum_{k>1} p_k^\mu\right) \frac{f(x_1, \mu_F) f(x_2, \mu_F)}{x_1 x_2 s} \left|\mathcal{M}_\alpha(p_k^\mu)\right|^2 W(\Phi'|\Phi_\alpha),$$

where: σ_α is the cross section; Φ' are the 4-momenta of the reconstructed particles; $d\Phi_\alpha$ is the element of phase space corresponding to parton-level variables with momentum conservation enforced [42]; $f(x, \mu_F)$ are the PDFs, where μ_F is the QCD factorization scale, computed using the NNPDF2.3LO set [43]; $|\mathcal{M}_\alpha|^2$ is the squared matrix element, computed with MAD-GRAPH5_aMC@NLO standalone [15] at LO accuracy, in a narrow-width approximation for the top quarks; and W are the transfer functions for jet energy and p_T^{miss}, relating parton-level variables to reconstructed quantities, evaluated from simulation studies and normalized to unity.

For all three processes, the mass of the W boson arising from the top quark decay follows a Breit–Wigner distribution, as specified in the matrix element. The virtual Z boson in the t$\bar{t}$Z hypothesis also follows a Breit–Wigner form, and interference with γ^* is included in the matrix element. The matrix element provided at LO in MADGRAPH5_aMC@NLO does not contain additional jets that are present in the data. To evaluate the matrix element at LO, the momentum of the tZq system must have a null transverse component. The tZq momentum is computed as the sum of the momenta of all particles from the tZq decay. An inverse boost corresponding to the opposite of the tZq p_T is applied to all final state particles, correcting thereby any recoiling jets not present in the LO matrix element.

In computing the MEM weights, jets with the highest CSVv2 discriminant values are assigned to the b quarks from top decays. Among the remaining jets, up to two jets with the highest $|\eta|$ (signal hypothesis), with invariant mass closest to the W boson mass (for the t$\bar{t}$Z hypothesis), or with the highest p_T (for the WZ+jets hypothesis), are assigned to the quarks at parton level. Jets in the 1bjet region may not be matched to all parton-level quarks needed in the t$\bar{t}$Z hypothesis (two b-quarks and two not-b quarks). In such cases, the t$\bar{t}$Z weight can still be computed by leaving the phase space of the missing jets unconstrained in the integral.

The final weight for each hypothesis α is taken as the average of the weights computed for each lepton and jet permutation. The MEM weights are combined in likelihood ratios of signal to the combination of t$\bar{t}$Z and WZ+jets in the 1bjet region and signal to t$\bar{t}$Z in the 2bjets region. These ratios are included as input variables to the BDT. In addition, the maximum value of the function being integrated is also included, corresponding to the MEM score associated to the most probable kinematic configuration. Eight variables were tested and five were retained for the training; the other three were excluded because they were highly correlated with other

variables or had a negligible discriminant power. The normalized BDT discriminators for signal and backgrounds in the 1bjet and 2bjets regions are shown in Fig. 2 for BDT trainings with and without MEM variables. Including the MEM variables improves the expected significance by about 20%.
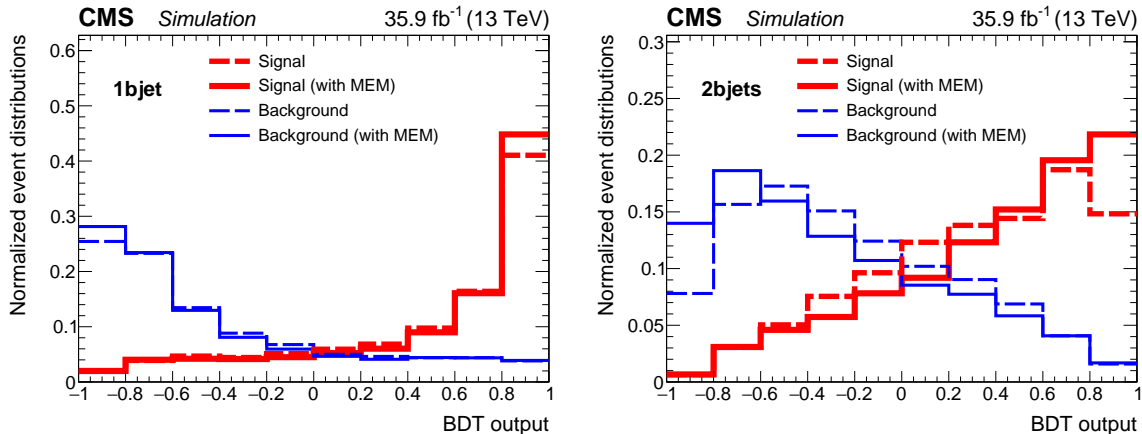

Figure 2: Normalized distributions of the BDT output for signal (thick lines) and backgrounds (thin lines) from simulation for the 1bjet (left) and 2bjets (right) regions. The discriminators including and excluding MEM variables in the BDT training are shown, respectively, as solid and dashed lines. Contributions from the four considered channels are included in the signals and backgrounds.

The predictions for some of the most discriminating variables in the BDT for the 1bjet and 2bjets regions are compared to data in Fig. 3. These variables are the largest CSVv2 discriminant value among all selected jets, the logarithm of the MEM score associated to the most probable tZq kinematic configuration, and the ΔR separation between the jet identified as a b quark and the recoiling jet. Figure 4 shows, for events in the 0bjet region, the η and p_T distributions of the recoiling jet, $\eta(j')$ and $p_T(j')$, and the asymmetry of the top quark decay lepton, defined as the product of its charge and pseudorapidity, $q_l|\eta(l)|$. The distributions in Figs. 3 and 4 are shown combined for the four channels: eee, eeμ, e$\mu\mu$, and $\mu\mu\mu$. The quadratic sum of the systematic and statistical uncertainties on the predictions is shown as a hatched band. The pulls of the distributions, defined in each bin as the difference between data and prediction, divided by the quadratic sum of total uncertainties in the predictions (systematic and statistical) and the data (statistical), are shown at the bottom of the plots.

The complete list of variables used in the two BDTs is given in Appendix A.

7 Systematic uncertainties

Different sources of systematic uncertainty can affect the number of events passing the selections, or the shape of the distributions used in the multivariate analysis.

The sources of systematic uncertainty considered correspond to:

- Luminosity: An uncertainty of 2.5% on the sample integrated luminosity [44] is propagated as a normalization-only uncertainty for the total predicted yields.
- Correction factors applied to the signal and simulated backgrounds:
  - Pileup: The number of simulated pileup events is corrected to match the measured number of events in data. The uncertainty on the total inelastic
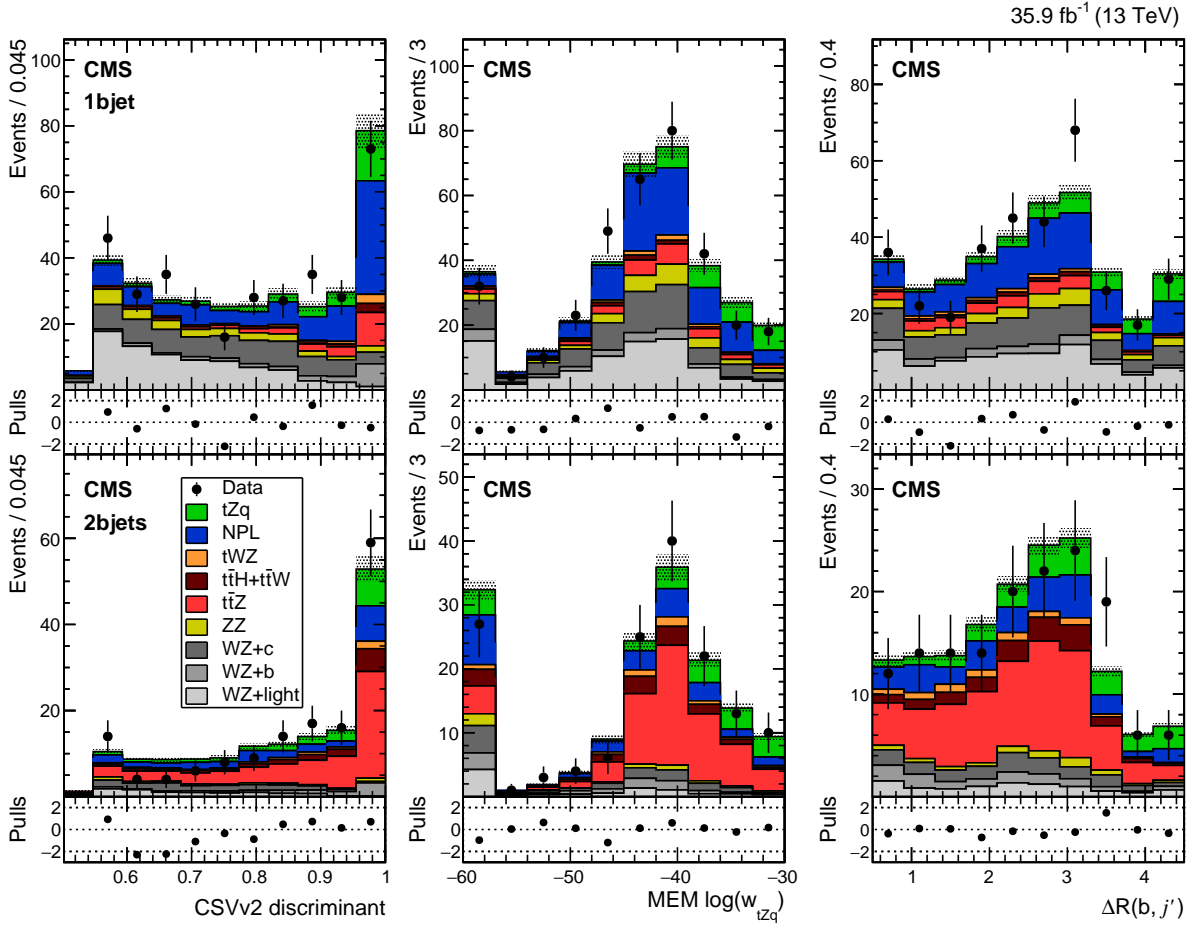
Figure 3: Data-to-prediction comparisons in the 1bjet region (signal-enriched, upper row) and in the 2bjets region (lower row) for the largest CSVv2 discriminant value among all selected jets (left), the logarithm of the MEM score associated to the most probable tZq kinematic configuration (centre), and the ΔR separation between the b quark and the recoiling jet (right). The distributions include events from all final states. Underflows and overflows are shown in the first and last bins, respectively. The predictions correspond to the normalizations obtained after the fit described in Section 8. The hatched bands include the total uncertainty on the background and signal contributions. The pulls in the distributions are shown in the bottom panels.

cross section is taken as 4.6%, and considered only in the shapes of the distributions.

- Trigger: The trigger efficiency is estimated to be near 100% both in data and in simulation. Variations in normalization of $\pm1\%$ ($\pm2\%$) are applied to the predicted yields in the $\mu\mu\mu$ and eeμ (e$\mu\mu$ and eee) channels to account for residual differences in trigger efficiency between data and simulation.

- Lepton selection: The factors used to correct the simulated distributions for lepton isolation and identification efficiencies are varied by their uncertainty, affecting both the shapes and the normalizations.

- Jet energy scale and resolution: The jet energy scale and resolution corrections are both varied by their uncertainty. The observed change is propagated to all related kinematic quantities, in particular $\vec{p}_T^{\text{miss}}$. These un-
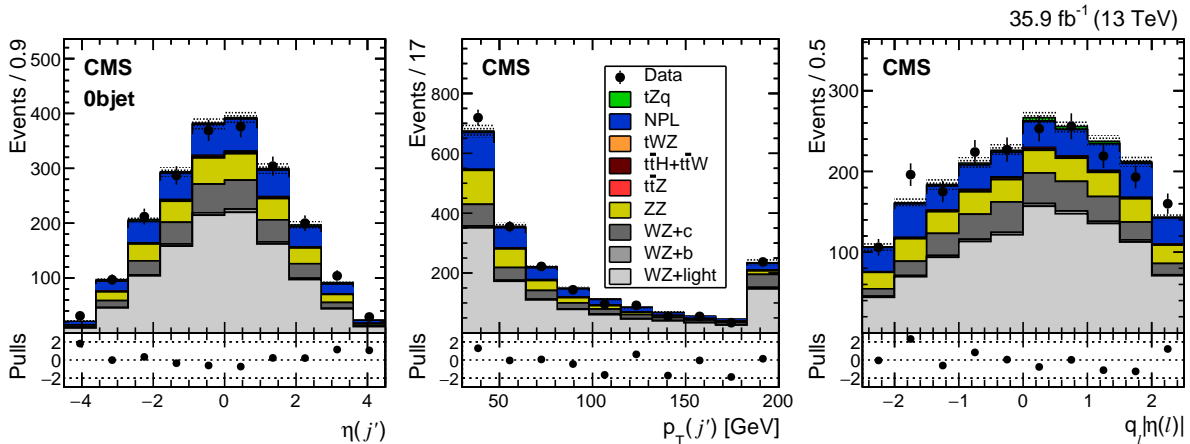
Figure 4: Data-to-prediction comparisons in the 0bjet region for the η (left) and p_T (centre) distributions of the recoiling jet, and for the asymmetry of the top quark decay lepton (right). More details are given in the caption of Fig. 3.

certainties affect both the shape and the normalization of the simulated distributions.

- b tagging: The scale factors related to b tagging and mistagging efficiencies are varied by one standard deviation. Eight independent changes are considered, including two types of statistical uncertainties on the b-, c-, and light-flavour components of the MC event samples, light-flavour contamination of the b tagging scale factors, and b quark contamination in the mistag scale factors. There is one "nuisance" parameter for each variation. Both shape and normalization are affected.

- The normalization of the simulated backgrounds: The input normalizations of all simulated background distributions are assumed to have a relative uncertainty of 30%. This reflects the theoretical uncertainties on the corresponding cross sections, scaled up by a factor of two or more, to account for possible limitations in the simulations in the phase space of the analysis.

- The NPL background estimation: The shape-related uncertainties on the backgrounds involving not-prompt leptons, determined with control samples in data, are estimated by varying the isolation criteria used to determine the NPL sample. The shape variations of not-prompt muons and electrons involve different nuisance parameters.

- The scale and PDF uncertainties for simulated signal (tZq) and background processes: These uncertainties affect the shape of the signal as well as the shape and normalization of the simulated background distributions, except for tWZ events, for which only normalization uncertainties from scales and PDF are considered.

  - The renormalization and factorization scales, at the matrix element level, are set to an identical value, which depends on the event generator and on the simulated processes. In particular, the scales for the simulated signal are set to $\sum \sqrt{(m^2 + p_T^2)}/2$, where the sum runs over all particles in the final state. The scales are varied up and down by a factor of 2.

  - The renormalization and factorization scales at the parton shower level, identical to the matrix element scales, are also varied by factors of 0.5 and 2; this uncertainty is only evaluated for the signal sample.

- The PDF uncertainties are evaluated by the root-mean-square of the results from 100 variations of the NNPDF set.

8   Results

The tool used for this statistical analysis [45] is based on the RooStats framework [46]. The analysis is performed beginning with a binned likelihood function

$$\mathcal{L}(\text{data}|\mu, \theta) = \sum_i \frac{\left[\mu s_i(\theta) + b_i(\theta) + \alpha_\text{e} B_i^\text{e}(\theta) + \alpha_\mu B_i^\mu(\theta)\right]^{N_i}}{N_i!} \text{e}^{-\mu s_i(\theta) - b_i(\theta) - \alpha_\text{e} B_i^\text{e}(\theta) - \alpha_\mu B_i^\mu(\theta)},$$

where N_i is the observed number of events in each bin, and $s_i(\theta)$ and $b_i(\theta)$ are the expected signal and background yields in each bin, respectively, normalized as discussed in the previous sections and taking into account all systematic uncertainties, represented by θ, as nuisance parameters associated with log-normal priors. The $B_i^{\text{e},\mu}(\theta)$ are the yields of NPL backgrounds, and the parameters $\alpha_{\text{e},\mu}$, which determine the normalization of the NPL backgrounds, are left free in the fit. The simultaneous fit to the data templates (BDT discriminators or m_T^W, depending on the region) in the four channels maximizes $\mathcal{L}(\text{data}|\mu, \theta)$, from which the measured cross section $\sigma(\text{t}\ell^+\ell^-\text{q})$ is extracted according to its relation to the signal strength

$$\mu = \frac{\sigma(\text{t}\ell^+\ell^-\text{q})}{\sigma^\text{SM}(\text{t}\ell^+\ell^-\text{q})},$$

where the cross section is defined for any decay of the top quark, and any decay of the Z boson to charged leptons. The reference cross section is $\sigma^\text{SM}(\text{t}\ell^+\ell^-\text{q}) = 94.2\,\text{fb}$, for $m_{\ell^+\ell^-} > 30\,\text{GeV}$. The measurement implies an extrapolation from the considered phase space (Section 5), defined as containing three leptons in the final state ($l'^+l'^-l$), and an additional constraint for $m_{\ell^+\ell^-}$ to be within $15\,\text{GeV}$ of the Z boson mass. The acceptance, defined as the fraction of $\text{t}\ell^+\ell^-\text{q}$ events fulfilling the event selection criteria, is estimated from the simulated tZq sample as 1.81%, combining the 1bjet, 2bjets, and 0bjet regions. All nuisance parameters are constrained in the fit.

The distributions resulting from the fit (post-fit) of the three variables used as templates in the measurement are shown in Fig. 5. Although the fit is performed for each channel, the figure displays the results combining the four channels.

Table 1 shows the results for the post-fit yields, separately for each channel, in the 1bjet region. The last two rows show the total number of predicted ("Total") and observed ("Data") events. The last column displays the ratio of the post-fit to pre-fit predictions, $N^\text{post-fit}/N^\text{pre-fit}$, accounting for the systematic uncertainties. The post-fit background normalizations are close to the pre-fit values for most of the background processes. The event yields for the WZ+light-flavour jets background preferred by the fit is significantly lower than the SM prediction. This feature, which might reflect the somewhat worse agreement between simulation and data for some bins of jet multiplicity [47], does not affect the measurement, as verified by the following checks. First, the predicted shapes of the kinematic variables relevant to the analysis are verified to describe the data in the WZ+light-flavour enriched region. The analysis is then repeated with the WZ+light-flavour normalization relative uncertainty increased to 50%, leaving the results unchanged within about half a percent. Finally, the WZ+light-flavour yield is fitted simultaneously with the NPL background yields using only the 0bjet region, and the resulting $N^\text{post-fit}/N^\text{pre-fit}$ scale factor is found to be 0.73 ± 0.11, in good agreement with the results of
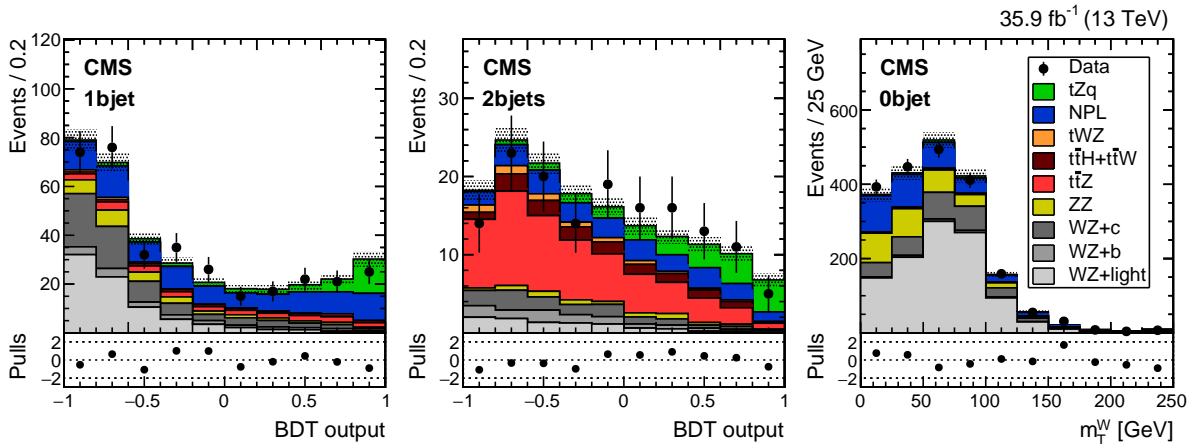
Figure 5: Template distributions used for signal extraction. Left: BDT discriminator in the 1bjet region; centre: BDT output in the 2bjets control region; right: m_T^W in the 0bjet control region. More details are given in the caption of Fig. 3.

Table 1. The post-fit number of tZq events in the 1bjet region is 32.3. The 0bjet and 2bjets control regions (not shown) also contain tZq events, with post-fit yields of ≈23 and 19 events, respectively.

Table 1: Observed and post-fit expected yields for each production process in the 1bjet region. The yields of columns 2–5 correspond to each channel, and column 6 displays the total for all channels. The last column displays the ratio between post-fit and pre-fit yields.

Process	eee	eeμ	e$\mu\mu$	$\mu\mu\mu$	All channels	$N^{\text{post-fit}}/N^{\text{pre-fit}}$
tZq	5.0 ± 1.5	6.6 ± 1.9	8.5 ± 2.5	12.3 ± 3.6	32.3 ± 5.0	—
t$\bar{\text{t}}$Z	3.7 ± 0.7	4.7 ± 0.9	6.1 ± 1.2	8.0 ± 1.5	22.4 ± 2.2	0.9 ± 0.2
t$\bar{\text{t}}$W	0.3 ± 0.1	0.3 ± 0.1	0.7 ± 0.2	0.6 ± 0.2	1.9 ± 0.3	1.0 ± 0.2
ZZ	4.8 ± 1.3	3.2 ± 0.9	9.0 ± 2.5	7.8 ± 2.2	24.7 ± 3.6	1.3 ± 0.3
WZ+b	3.0 ± 0.9	3.4 ± 1.1	4.6 ± 1.4	5.5 ± 1.7	16.6 ± 2.6	1.0 ± 0.2
WZ+c	9.0 ± 2.4	13.7 ± 3.7	18.0 ± 4.9	24.2 ± 6.5	64.8 ± 9.3	1.0 ± 0.2
WZ+light	12.2 ± 1.6	16.6 ± 2.0	22.4 ± 2.8	29.1 ± 3.4	80.3 ± 5.1	0.7 ± 0.1
t$\bar{\text{t}}$H	0.6 ± 0.2	0.9 ± 0.3	1.0 ± 0.3	1.5 ± 0.4	4.0 ± 0.6	1.0 ± 0.2
tWZ	1.0 ± 0.3	1.3 ± 0.4	1.7 ± 0.5	2.4 ± 0.7	6.5 ± 1.0	1.0 ± 0.2
NPL: electrons	19.2 ± 3.1	0.6 ± 0.1	17.9 ± 2.8	—	37.7 ± 4.2	—
NPL: muons	—	7.2 ± 2.3	31.1 ± 9.9	15.3 ± 4.9	53.6 ± 11.3	—
Total	58.8 ± 4.8	58.4 ± 5.5	121 ± 12	107 ± 10	345 ± 18	
Data	56	58	104	125	343	

The observed tZq signal strength is

$$\mu = 1.31^{+0.35}_{-0.33}\,(\text{stat})^{+0.31}_{-0.25}\,(\text{syst}),$$

from which, using the reference NLO cross section, the measured cross section is found to be

$$\sigma(\text{t}\ell^+\ell^-\text{q}) = 123^{+33}_{-31}\,(\text{stat})^{+29}_{-23}\,(\text{syst})\,\text{fb},$$

for $m_{\ell^+\ell^-} > 30\,\text{GeV}$, where ℓ stands for electrons, muons, and τ leptons. The best-fit signal strength and cross section, as well as an approximate 68% CL interval, are extracted following the profile likelihood scan procedure described in Ref. [48]. The fit is redone without including

the systematic uncertainties, to evaluate the statistical uncertainty of the result. The quoted systematic uncertainty is then calculated as the difference in quadrature between the 68% CL intervals obtained in the nominal fit and in the fit without systematic uncertainties. The precision of the measurement is limited by the statistical uncertainty. Among the systematic uncertainties, the dominating ones arise from the normalization of the NPL background (left free in the fit), the scale dependence at the parton shower level, the b tagging efficiency, and the normalization of the $t\bar{t}Z$ background. The corresponding observed (expected) significance against the background-only hypothesis is 3.7 (3.1) standard deviations, with an observed statistical p-value of 0.0001. The expected significance is estimated from an Asimov toy dataset [49]. The 68% CL interval of the expected significance is 1.4–5.9.

Potential biases from the background yields used as input have been searched for. First, the analysis was repeated to measure simultaneously the tZq and $t\bar{t}Z$ cross sections, in addition to determining the NPL background normalization. The tZq signal strength increases by less than 1%, whereas the observed and expected significances decrease by about 1%. Then, the not-prompt muon and electron normalizations are set to their input values, described as the first step in Section 6.2, and allowed to vary in the fit as Gaussian constraints of 100% uncertainty. In this case, both the tZq signal strength and the significances increase by about 10%, while the uncertainties on the signal strength increase by about 5%. In addition, the measurement is repeated in each channel, and the measured signal strengths are found to be $1.32^{+1.14}_{-0.99}$, $0.66^{+0.78}_{-0.63}$, $0.01^{+0.97}_{-0.01}$, and $1.22^{+0.75}_{-0.63}$ for the eee, eeμ, e$\mu\mu$, and $\mu\mu\mu$ channels, respectively. The highest observed (expected) significance is 2.1 (1.9) standard deviations in the $\mu\mu\mu$ channel. Finally, the results were verified in a counting analysis, using the yields observed in control regions selected using similar criteria to those of the 1bjet, 2bjets, and 0bjet regions. The simulated backgrounds are normalized according to their SM predictions, while the normalization of the NPL contributions follows the procedure described in Section 6.2 as the first step of the NPL normalization in the shape analysis. The results from the counting and shape analyses are in agreement.

9   Summary

The associated production cross section of a single top quark and a Z boson was measured using data from pp collisions at 13 TeV collected by the CMS experiment, corresponding to an integrated luminosity of 35.9 fb^{-1}. The measurement uses events containing three charged leptons in the final state. Evidence for tZq production is found with an observed (expected) significance of 3.7 (3.1) standard deviations. The cross section is measured to be $\sigma(t\ell^+\ell^-q) = 123^{+33}_{-31}\,\text{(stat)}^{+29}_{-23}\,\text{(syst)}\,\text{fb}$, for $m_{\ell^+\ell^-} > 30\,\text{GeV}$, where ℓ stands for electrons, muons, or τ leptons. This value is compatible with the next-to-leading-order standard model prediction of 94.2 ± 3.1 fb.

Acknowledgments

References

[1] CDF and D0 Collaborations, "Tevatron combination of single-top-quark cross sections and determination of the magnitude of the Cabibbo-Kobayashi-Maskawa matrix element V_{tb}", *Phys. Rev. Lett.* **115** (2015) 152003, `doi:10.1103/PhysRevLett.115.152003`, `arXiv:1503.05027`.

[2] CDF and D0 Collaborations, "Observation of s-channel production of single top quarks at the Tevatron", *Phys. Rev. Lett.* **112** (2014) 231803, `doi:10.1103/PhysRevLett.112.231803`, `arXiv:1402.5126`.

[3] ATLAS Collaboration, "Comprehensive measurements of t-channel single top-quark production cross sections at $\sqrt{s} = 7$ TeV with the ATLAS detector", *Phys. Rev. D* **90** (2014) 112006, `doi:10.1103/PhysRevD.90.112006`, `arXiv:1406.7844`.

[4] ATLAS Collaboration, "Measurement of the production cross section of a single top quark in association with a W boson at 8 TeV with the ATLAS experiment", *JHEP* **01** (2016) 064, `doi:10.1007/JHEP01(2016)064`, `arXiv:1510.03752`.

[5] ATLAS Collaboration, "Evidence for single top-quark production in the *s*-channel in proton-proton collisions at $\sqrt{s}$ = 8 TeV with the ATLAS detector using the Matrix Element Method", *Phys. Lett. B* **756** (2016) 228, `doi:10.1016/j.physletb.2016.03.017`, `arXiv:1511.05980`.

[6] ATLAS Collaboration, "Measurement of the inclusive cross-sections of single top-quark and top-antiquark *t*-channel production in pp collisions at $\sqrt{s}$ = 13 TeV with the ATLAS detector", *JHEP* **04** (2017) 086, `doi:10.1007/JHEP04(2017)086`, `arXiv:1609.03920`.

[7] ATLAS Collaboration, "Measurement of the cross-section for producing a W boson in association with a single top quark in pp collisions at $\sqrt{s}$ = 13 TeV with ATLAS", *JHEP* **01** (2018) 063, `doi:10.1007/JHEP01(2018)063`, `arXiv:1612.07231`.

[8] CMS Collaboration, "Measurement of the single-top-quark *t*-channel cross section in pp collisions at $\sqrt{s}$ = 7 TeV", *JHEP* **12** (2012) 035, `doi:10.1007/JHEP12(2012)035`, `arXiv:1209.4533`.

[9] CMS Collaboration, "Observation of the associated production of a single top quark and a W boson in pp collisions at $\sqrt{s}$ = 8 TeV", *Phys. Rev. Lett.* **112** (2014) 231802, `doi:10.1103/PhysRevLett.112.231802`, `arXiv:1401.2942`.

[10] CMS Collaboration, "Search for *s*-channel single top quark production in pp collisions at $\sqrt{s}$ = 7 and 8 TeV", *JHEP* **09** (2016) 027, `doi:10.1007/JHEP09(2016)027`, `arXiv:1603.02555`.

[11] CMS Collaboration, "Cross section measurement of *t*-channel single top quark production in pp collisions at $\sqrt{s}$ = 13 TeV", *Phys. Lett. B* **72** (2017) 752, `doi:10.1016/j.physletb.2017.07.047`, `arXiv:1610.00678`.

[12] J. A. Aguilar-Saavedra, "Top flavor-changing neutral interactions: Theoretical expectations and experimental detection", in *Particle physics phenomenology at high energy colliders. Proceedings, Final meeting of the European Union Network, Montpellier, France, September 26-27, 2004*, volume 35, p. 2695. 2004. `arXiv:hep-ph/0409342`. [Acta Phys. Polon. B 35 (2004) 2695].

[13] J.-L. Agram et al., "Probing top anomalous couplings at the LHC with trilepton signatures in the single top mode", *Phys. Lett. B* **725** (2013) 123, `doi:10.1016/j.physletb.2013.06.052`, `arXiv:1304.5551`.

[14] S. L. Glashow, J. Iliopoulos, and L. Maiani, "Weak interactions with lepton hadron symmetry", *Phys. Rev. D* **2** (1970) 1285, `doi:10.1103/PhysRevD.2.1285`.

[15] J. Alwall et al., "The automated computation of tree-level and next-to-leading order differential cross sections, and their matching to parton shower simulations", *JHEP* **07** (2014) 079, `doi:10.1007/JHEP07(2014)079`, `arXiv:1405.0301`.

[16] NNPDF Collaboration, "Parton distributions for the LHC Run II", *JHEP* **04** (2015) 040, `doi:10.1007/JHEP04(2015)040`, `arXiv:1410.8849`.

[17] J. Campbell, R. K. Ellis, and R. Roentsch, "Single top production in association with a Z boson at the LHC", *Phys. Rev. D* **87** (2013) 114006, `doi:10.1103/PhysRevD.87.114006`, `arXiv:1302.3856`.

[18] CMS Collaboration, "Search for associated production of a Z boson with a single top quark and for tZ flavour-changing interactions in pp collisions at $\sqrt{s} = 8$ TeV", *JHEP* **07** (2017) 003, `doi:10.1007/JHEP07(2017)003`, `arXiv:1702.01404`.

[19] ATLAS Collaboration, "Measurement of the production cross-section of a single top quark in association with a Z boson in proton-proton collisions at 13 TeV with the ATLAS detector", (2017). `arXiv:1710.03659`.

[20] L. Breiman, J. Friedman, C. J. Stone, and R. A. Olshen, "Classification and Regression Trees". Chapman & Hall, New York, 1984.

[21] CMS Collaboration, "Performance of electron reconstruction and selection with the CMS detector in proton-proton collisions at $\sqrt{s} = 8$ TeV", *JINST* **10** (2015) P06005, `doi:10.1088/1748-0221/10/06/P06005`, `arXiv:1502.02701`.

[22] CMS Collaboration, "Performance of CMS muon reconstruction in pp collision events at $\sqrt{s} = 7$ TeV", *JINST* **7** (2012) P10002, `doi:10.1088/1748-0221/7/10/P10002`, `arXiv:1206.4071`.

[23] CMS Collaboration, "The CMS experiment at the CERN LHC", *JINST* **3** (2008) S08004, `doi:10.1088/1748-0221/3/08/S08004`.

[24] CMS Collaboration, "The CMS trigger system", *JINST* **12** (2017) P01020, `doi:10.1088/1748-0221/12/01/P01020`, `arXiv:1609.02366`.

[25] CMS Collaboration, "Particle-flow reconstruction and global event description with the CMS detector", *JINST* **12** (2017) P10003, `doi:10.1088/1748-0221/12/10/P10003`, `arXiv:1706.04965`.

[26] M. Cacciari, G. P. Salam, and G. Soyez, "The anti-k_t jet clustering algorithm", *JHEP* **04** (2008) 063, `doi:10.1088/1126-6708/2008/04/063`, `arXiv:0802.1189`.

[27] M. Cacciari, G. P. Salam, and G. Soyez, "FastJet user manual", *Eur. Phys. J. C* **72** (2012) 1896, `doi:10.1140/epjc/s10052-012-1896-2`, `arXiv:1111.6097`.

[28] CMS Collaboration, "Jet energy scale and resolution in the CMS experiment in pp collisions at 8 TeV", *JINST* **12** (2017) P02014, `doi:10.1088/1748-0221/12/02/P02014`, `arXiv:1607.03663`.

[29] CMS Collaboration, "Identification of b-quark jets with the CMS experiment", *JINST* **8** (2013) P04013, `doi:10.1088/1748-0221/8/04/P04013`.

[30] CMS Collaboration, "Identification of b quark jets at the CMS Experiment in the LHC Run 2", CMS Physics Analysis Summary CMS-PAS-BTV-15-001, 2016.

[31] P. Nason, "A new method for combining NLO QCD with shower Monte Carlo algorithms", *JHEP* **11** (2004) 040, `doi:10.1088/1126-6708/2004/11/040`, `arXiv:hep-ph/0409146`.

[32] S. Frixione, P. Nason, and C. Oleari, "Matching NLO QCD computations with parton shower simulations: the POWHEG method", *JHEP* **11** (2007) 070, `doi:10.1088/1126-6708/2007/11/070`, `arXiv:0709.2092`.

[33] S. Alioli, P. Nason, C. Oleari, and E. Re, "A general framework for implementing NLO calculations in shower Monte Carlo programs: the POWHEG BOX", *JHEP* **06** (2010) 043, `doi:10.1007/JHEP06(2010)043`, `arXiv:1002.2581`.

[34] E. Re, "Single-top *Wt*-channel- production matched with parton showers using the POWHEG method", *Eur. Phys. J. C* **71** (2011) 1547, `doi:10.1140/epjc/s10052-011-1547-z`, `arXiv:1009.2450`.

[35] S. Alioli, P. Nason, C. Oleari, and E. Re, "NLO single-top production matched with shower in POWHEG: *s*- and *t*-channel contributions", *JHEP* **09** (2009) 111, `doi:10.1088/1126-6708/2009/09/111`, `arXiv:0907.4076`. [Erratum: `doi:10.1007/JHEP02(2010)011`].

[36] T. Melia, P. Nason, R. Rontsch, and G. Zanderighi, "W^+W^-, WZ and ZZ production in the POWHEG BOX", *JHEP* **11** (2011) 078, `doi:10.1007/JHEP11(2011)078`, `arXiv:1107.5051`.

[37] T. Sjöstrand et al., "An introduction to PYTHIA 8.2", *Comput. Phys. Commun.* **191** (2015) 159, `doi:10.1016/j.cpc.2015.01.024`, `arXiv:1410.3012`.

[38] CMS Collaboration, "Event generator tunes obtained from underlying event and multiparton scattering measurements", *Eur. Phys. J. C* **76** (2016) 155, `doi:10.1140/epjc/s10052-016-3988-x`, `arXiv:1512.00815`.

[39] GEANT4 Collaboration, "GEANT4: A simulation toolkit", *Nucl. Instrum. Meth. A* **506** (2003) 250, `doi:10.1016/S0168-9002(03)01368-8`.

[40] H. Voss, A. Höcker, J. Stelzer, and F. Tegenfeldt, "TMVA, the toolkit for multivariate data analysis with ROOT", in *XIth International Workshop on Advanced Computing and Analysis Techniques in Physics Research (ACAT)*, p. 40. 2007. `arXiv:physics/0703039`.

[41] D0 Collaboration, "A precision measurement of the mass of the top quark", *Nature* **429** (2004) 638, `doi:10.1038/nature02589`, `arXiv:hep-ex/0406031`.

[42] P. Artoisenet, V. Lemaitre, F. Maltoni, and O. Mattelaer, "Automation of the matrix element reweighting method", *JHEP* **12** (2010) 068, `doi:10.1007/JHEP12(2010)068`, `arXiv:1007.3300`.

[43] NNPDF Collaboration, "Parton distributions with LHC data", *Nucl. Phys. B* **867** (2013) 244, `doi:10.1016/j.nuclphysb.2012.10.003`, `arXiv:1207.1303`.

[44] CMS Collaboration, "CMS luminosity measurement for the 2015 data taking period", CMS Physics Analysis Summary CMS-PAS-LUM-15-001, 2016.

[45] ATLAS and CMS Collaborations, "Procedure for the LHC Higgs boson search combination in Summer 2011", Joint CMS and ATLAS note CMS-NOTE-2011-005; ATL-PHYS-PUB-2011-11, 2011.

[46] L. Moneta et al., "The RooStats Project", in *Proc. of the 13th International Workshop on Advanced Computing and Analysis Techniques in Physics Research (ACAT2010)*. SISSA, 2010. `arXiv:1009.1003`. PoS(ACAT2010)057.

[47] CMS Collaboration, "Measurement of the WZ production cross section in pp collisions at $\sqrt{s} = 13$ TeV", *Phys. Lett. B* **766** (2017) 268, `doi:10.1016/j.physletb.2017.01.011`, `arXiv:1607.06943`.

[48] CMS Collaboration, "Precise determination of the mass of the Higgs boson and tests of compatibility of its couplings with the standard model predictions using proton collisions at 7 and 8 TeV", *Eur. Phys. J. C* **75** (2015) 212, `doi:10.1140/epjc/s10052-015-3351-7`, `arXiv:1412.8662`.

[49] G. Cowan, K. Cranmer, E. Gross, and O. Vitells, "Asymptotic formulae for likelihood-based tests of new physics", *Eur. Phys. J. C* **71** (2011) 1554, `doi:10.1140/epjc/s10052-011-1554-0`, `arXiv:1007.1727`.

A Variables used in the shape analysis

A short description of the variables used in the Boosted Decision Trees in the 1bjet and 2bjets regions is given in Table 2. The BDTs in the 1bjet region and 2bjets region used 16 and 15 variables each, respectively, 10 of which common to the two regions (variables 1–9 and 17 in Table 2). From the total of 21 variables, 16 are related to the kinematic quantities associated to the final state objects (1–16 in Table 2), while five of them are related to the MEM (17–21 in Table 2).

Table 2: Description of the variables used in the BDTs. The symbol Y (N) in the third and fourth columns indicates that the variable was (was not) used in the 1bjet and 2bjets BDTs.

	Variable description	1bjet	2bjets
1	CSVv2 algorithm discriminant	Y	Y
2	ΔR separation between the jet identified as a b quark and the recoiling jet	Y	Y
3	η of the recoiling jet	Y	Y
4	p_T of the recoiling jet	Y	Y
5	η of the Z boson	Y	Y
6	Top quark mass	Y	Y
7	ΔR separation between the top quark decay lepton and the jet closest to it	Y	Y
8	Top quark decay lepton asymmetry	Y	Y
9	Azimuth angle separation between the top quark decay lepton and the Z boson	Y	Y
10	Azimuth angle separation between the top quark decay lepton and the b quark	Y	N
11	η of the top quark decay lepton	Y	N
12	η of the jet with highest p_T	Y	N
13	ΔR separation between the top quark decay lepton and the recoil jet	N	Y
14	ΔR separation between the Z boson and the top quark	N	Y
15	p_T of the Z boson	N	Y
16	Number of b tagged jets	N	Y
17	Logarithm of the MEM score associated to the most probable tZq kinematic configuration	Y	Y
18	Logarithm of the MEM score associated to the most probable $\mathrm{t\bar{t}Z}$ kinematic configuration	N	Y
19	Log-likelihood ratio of the tZq hypothesis against the $\mathrm{t\bar{t}Z}$ hypothesis	Y	N
20	Log-likelihood ratio of the tZq hypothesis against the $\mathrm{t\bar{t}Z}$ hypothesis with $\mathrm{t\bar{t}Z}$ and tZq weights rescaled such that their mean values are similar	Y	N
21	Log-likelihood ratio of the MEM weights for $\mathrm{t\bar{t}Z}$ against $\mathrm{t\bar{t}Z}$ +WZ hypothesis	Y	N

B The CMS Collaboration

Yerevan Physics Institute, Yerevan, Armenia
A.M. Sirunyan, A. Tumasyan

Institut für Hochenergiephysik, Wien, Austria
W. Adam, F. Ambrogi, E. Asilar, T. Bergauer, J. Brandstetter, E. Brondolin, M. Dragicevic, J. Erö, A. Escalante Del Valle, M. Flechl, M. Friedl, R. Frühwirth[1], V.M. Ghete, J. Grossmann, J. Hrubec, M. Jeitler[1], A. König, N. Krammer, I. Krätschmer, D. Liko, T. Madlener, I. Mikulec, E. Pree, N. Rad, H. Rohringer, J. Schieck[1], R. Schöfbeck, M. Spanring, D. Spitzbart, A. Taurok, W. Waltenberger, J. Wittmann, C.-E. Wulz[1], M. Zarucki

Institute for Nuclear Problems, Minsk, Belarus
V. Chekhovsky, V. Mossolov, J. Suarez Gonzalez

Universiteit Antwerpen, Antwerpen, Belgium
E.A. De Wolf, D. Di Croce, X. Janssen, J. Lauwers, M. Van De Klundert, H. Van Haevermaet, P. Van Mechelen, N. Van Remortel

Vrije Universiteit Brussel, Brussel, Belgium
S. Abu Zeid, F. Blekman, J. D'Hondt, I. De Bruyn, J. De Clercq, K. Deroover, G. Flouris, D. Lontkovskyi, S. Lowette, I. Marchesini, S. Moortgat, L. Moreels, Q. Python, K. Skovpen, S. Tavernier, W. Van Doninck, P. Van Mulders, I. Van Parijs

Université Libre de Bruxelles, Bruxelles, Belgium
D. Beghin, B. Bilin, H. Brun, B. Clerbaux, G. De Lentdecker, H. Delannoy, B. Dorney, G. Fasanella, L. Favart, R. Goldouzian, A. Grebenyuk, A.K. Kalsi, T. Lenzi, J. Luetic, T. Maerschalk, A. Marinov, T. Seva, E. Starling, C. Vander Velde, P. Vanlaer, D. Vannerom, R. Yonamine, F. Zenoni

Ghent University, Ghent, Belgium
T. Cornelis, D. Dobur, A. Fagot, M. Gul, I. Khvastunov[2], D. Poyraz, C. Roskas, S. Salva, D. Trocino, M. Tytgat, W. Verbeke, M. Vit, N. Zaganidis

Université Catholique de Louvain, Louvain-la-Neuve, Belgium
H. Bakhshiansohi, O. Bondu, S. Brochet, G. Bruno, C. Caputo, A. Caudron, P. David, S. De Visscher, C. Delaere, M. Delcourt, B. Francois, A. Giammanco, M. Komm, G. Krintiras, V. Lemaitre, A. Magitteri, A. Mertens, M. Musich, K. Piotrzkowski, L. Quertenmont, A. Saggio, M. Vidal Marono, S. Wertz, J. Zobec

Centro Brasileiro de Pesquisas Fisicas, Rio de Janeiro, Brazil
W.L. Aldá Júnior, F.L. Alves, G.A. Alves, L. Brito, G. Correia Silva, C. Hensel, A. Moraes, M.E. Pol, P. Rebello Teles

Universidade do Estado do Rio de Janeiro, Rio de Janeiro, Brazil
E. Belchior Batista Das Chagas, W. Carvalho, J. Chinellato[3], E. Coelho, E.M. Da Costa, G.G. Da Silveira[4], D. De Jesus Damiao, S. Fonseca De Souza, L.M. Huertas Guativa, H. Malbouisson, M. Melo De Almeida, C. Mora Herrera, L. Mundim, H. Nogima, L.J. Sanchez Rosas, A. Santoro, A. Sznajder, M. Thiel, E.J. Tonelli Manganote[3], F. Torres Da Silva De Araujo, A. Vilela Pereira

Universidade Estadual Paulista [a], Universidade Federal do ABC [b], São Paulo, Brazil
S. Ahuja[a], C.A. Bernardes[a], T.R. Fernandez Perez Tomei[a], E.M. Gregores[b], P.G. Mercadante[b], S.F. Novaes[a], Sandra S. Padula[a], D. Romero Abad[b], J.C. Ruiz Vargas[a]

Institute for Nuclear Research and Nuclear Energy, Bulgarian Academy of Sciences, Sofia, Bulgaria
A. Aleksandrov, R. Hadjiiska, P. Iaydjiev, M. Misheva, M. Rodozov, M. Shopova, G. Sultanov

University of Sofia, Sofia, Bulgaria
A. Dimitrov, L. Litov, B. Pavlov, P. Petkov

Beihang University, Beijing, China
W. Fang[5], X. Gao[5], L. Yuan

Institute of High Energy Physics, Beijing, China
M. Ahmad, J.G. Bian, G.M. Chen, H.S. Chen, M. Chen, Y. Chen, C.H. Jiang, D. Leggat, H. Liao, Z. Liu, F. Romeo, S.M. Shaheen, A. Spiezia, J. Tao, C. Wang, Z. Wang, E. Yazgan, H. Zhang, J. Zhao

State Key Laboratory of Nuclear Physics and Technology, Peking University, Beijing, China
Y. Ban, G. Chen, J. Li, Q. Li, S. Liu, Y. Mao, S.J. Qian, D. Wang, Z. Xu, F. Zhang[5]

Tsinghua University, Beijing, China
Y. Wang

Universidad de Los Andes, Bogota, Colombia
C. Avila, A. Cabrera, C.A. Carrillo Montoya, L.F. Chaparro Sierra, C. Florez, C.F. González Hernández, J.D. Ruiz Alvarez, M.A. Segura Delgado

University of Split, Faculty of Electrical Engineering, Mechanical Engineering and Naval Architecture, Split, Croatia
B. Courbon, N. Godinovic, D. Lelas, I. Puljak, P.M. Ribeiro Cipriano, T. Sculac

University of Split, Faculty of Science, Split, Croatia
Z. Antunovic, M. Kovac

Institute Rudjer Boskovic, Zagreb, Croatia
V. Brigljevic, D. Ferencek, K. Kadija, B. Mesic, A. Starodumov[6], T. Susa

University of Cyprus, Nicosia, Cyprus
M.W. Ather, A. Attikis, G. Mavromanolakis, J. Mousa, C. Nicolaou, F. Ptochos, P.A. Razis, H. Rykaczewski

Charles University, Prague, Czech Republic
M. Finger[7], M. Finger Jr.[7]

Universidad San Francisco de Quito, Quito, Ecuador
E. Carrera Jarrin

Academy of Scientific Research and Technology of the Arab Republic of Egypt, Egyptian Network of High Energy Physics, Cairo, Egypt
Y. Assran[8,9], M.A. Mahmoud[10,9], A. Mahrous[11]

National Institute of Chemical Physics and Biophysics, Tallinn, Estonia
S. Bhowmik, R.K. Dewanjee, M. Kadastik, L. Perrini, M. Raidal, C. Veelken

Department of Physics, University of Helsinki, Helsinki, Finland
P. Eerola, H. Kirschenmann, J. Pekkanen, M. Voutilainen

Helsinki Institute of Physics, Helsinki, Finland
J. Havukainen, J.K. Heikkilä, T. Järvinen, V. Karimäki, R. Kinnunen, T. Lampén, K. Lassila-Perini, S. Laurila, S. Lehti, T. Lindén, P. Luukka, T. Mäenpää, H. Siikonen, E. Tuominen, J. Tuominiemi

Lappeenranta University of Technology, Lappeenranta, Finland
T. Tuuva

IRFU, CEA, Université Paris-Saclay, Gif-sur-Yvette, France
M. Besancon, F. Couderc, M. Dejardin, D. Denegri, J.L. Faure, F. Ferri, S. Ganjour, S. Ghosh, A. Givernaud, P. Gras, G. Hamel de Monchenault, P. Jarry, C. Leloup, E. Locci, M. Machet, J. Malcles, G. Negro, J. Rander, A. Rosowsky, M.Ö. Sahin, M. Titov

Laboratoire Leprince-Ringuet, Ecole polytechnique, CNRS/IN2P3, Université Paris-Saclay, Palaiseau, France
A. Abdulsalam[12], C. Amendola, I. Antropov, S. Baffioni, F. Beaudette, P. Busson, L. Cadamuro, C. Charlot, R. Granier de Cassagnac, M. Jo, I. Kucher, S. Lisniak, A. Lobanov, J. Martin Blanco, M. Nguyen, C. Ochando, G. Ortona, P. Paganini, P. Pigard, R. Salerno, J.B. Sauvan, Y. Sirois, A.G. Stahl Leiton, T. Strebler, Y. Yilmaz, A. Zabi, A. Zghiche

Université de Strasbourg, CNRS, IPHC UMR 7178, F-67000 Strasbourg, France
J.-L. Agram[13], J. Andrea, D. Bloch, J.-M. Brom, M. Buttignol, E.C. Chabert, N. Chanon, C. Collard, E. Conte[13], X. Coubez, F. Drouhin[13], J.-C. Fontaine[13], D. Gelé, U. Goerlach, M. Jansová, P. Juillot, A.-C. Le Bihan, N. Tonon, P. Van Hove

Centre de Calcul de l'Institut National de Physique Nucleaire et de Physique des Particules, CNRS/IN2P3, Villeurbanne, France
S. Gadrat

Université de Lyon, Université Claude Bernard Lyon 1, CNRS-IN2P3, Institut de Physique Nucléaire de Lyon, Villeurbanne, France
S. Beauceron, C. Bernet, G. Boudoul, R. Chierici, D. Contardo, P. Depasse, H. El Mamouni, J. Fay, L. Finco, S. Gascon, M. Gouzevitch, G. Grenier, B. Ille, F. Lagarde, I.B. Laktineh, M. Lethuillier, L. Mirabito, A.L. Pequegnot, S. Perries, A. Popov[14], V. Sordini, M. Vander Donckt, S. Viret, S. Zhang

Georgian Technical University, Tbilisi, Georgia
T. Toriashvili[15]

Tbilisi State University, Tbilisi, Georgia
Z. Tsamalaidze[7]

RWTH Aachen University, I. Physikalisches Institut, Aachen, Germany
C. Autermann, L. Feld, M.K. Kiesel, K. Klein, M. Lipinski, M. Preuten, C. Schomakers, J. Schulz, M. Teroerde, B. Wittmer, V. Zhukov[14]

RWTH Aachen University, III. Physikalisches Institut A, Aachen, Germany
A. Albert, D. Duchardt, M. Endres, M. Erdmann, S. Erdweg, T. Esch, R. Fischer, A. Güth, T. Hebbeker, C. Heidemann, K. Hoepfner, S. Knutzen, M. Merschmeyer, A. Meyer, P. Millet, S. Mukherjee, T. Pook, M. Radziej, H. Reithler, M. Rieger, F. Scheuch, D. Teyssier, S. Thüer

RWTH Aachen University, III. Physikalisches Institut B, Aachen, Germany
G. Flügge, B. Kargoll, T. Kress, A. Künsken, T. Müller, A. Nehrkorn, A. Nowack, C. Pistone, O. Pooth, A. Stahl[16]

Deutsches Elektronen-Synchrotron, Hamburg, Germany
M. Aldaya Martin, T. Arndt, C. Asawatangtrakuldee, K. Beernaert, O. Behnke, U. Behrens, A. Bermúdez Martínez, A.A. Bin Anuar, K. Borras[17], V. Botta, A. Campbell, P. Connor, C. Contreras-Campana, F. Costanza, C. Diez Pardos, G. Eckerlin, D. Eckstein, T. Eichhorn, E. Eren, E. Gallo[18], J. Garay Garcia, A. Geiser, J.M. Grados Luyando, A. Grohsjean, P. Gunnellini, M. Guthoff, A. Harb, J. Hauk, M. Hempel[19], H. Jung, M. Kasemann, J. Keaveney, C. Kleinwort, I. Korol, D. Krücker, W. Lange, A. Lelek, T. Lenz, K. Lipka, W. Lohmann[19], R. Mankel, I.-A. Melzer-Pellmann, A.B. Meyer, M. Missiroli, G. Mittag, J. Mnich, A. Mussgiller, E. Ntomari, D. Pitzl, A. Raspereza, M. Savitskyi, P. Saxena, R. Shevchenko, N. Stefaniuk, G.P. Van Onsem, R. Walsh, Y. Wen, K. Wichmann, C. Wissing, O. Zenaiev

University of Hamburg, Hamburg, Germany
R. Aggleton, S. Bein, V. Blobel, M. Centis Vignali, T. Dreyer, E. Garutti, D. Gonzalez, J. Haller, A. Hinzmann, M. Hoffmann, A. Karavdina, R. Klanner, R. Kogler, N. Kovalchuk, S. Kurz, D. Marconi, M. Meyer, M. Niedziela, D. Nowatschin, F. Pantaleo[16], T. Peiffer, A. Perieanu, C. Scharf, P. Schleper, A. Schmidt, S. Schumann, J. Schwandt, J. Sonneveld, H. Stadie, G. Steinbrück, F.M. Stober, M. Stöver, H. Tholen, D. Troendle, E. Usai, A. Vanhoefer, B. Vormwald

Institut für Experimentelle Kernphysik, Karlsruhe, Germany
M. Akbiyik, C. Barth, M. Baselga, S. Baur, E. Butz, R. Caspart, T. Chwalek, F. Colombo, W. De Boer, A. Dierlamm, N. Faltermann, B. Freund, R. Friese, M. Giffels, M.A. Harrendorf, F. Hartmann[16], S.M. Heindl, U. Husemann, F. Kassel[16], S. Kudella, H. Mildner, M.U. Mozer, Th. Müller, M. Plagge, G. Quast, K. Rabbertz, M. Schröder, I. Shvetsov, G. Sieber, H.J. Simonis, R. Ulrich, S. Wayand, M. Weber, T. Weiler, S. Williamson, C. Wöhrmann, R. Wolf

Institute of Nuclear and Particle Physics (INPP), NCSR Demokritos, Aghia Paraskevi, Greece
G. Anagnostou, G. Daskalakis, T. Geralis, A. Kyriakis, D. Loukas, I. Topsis-Giotis

National and Kapodistrian University of Athens, Athens, Greece
G. Karathanasis, S. Kesisoglou, A. Panagiotou, N. Saoulidou, E. Tziaferi

National Technical University of Athens, Athens, Greece
K. Kousouris

University of Ioánnina, Ioánnina, Greece
I. Evangelou, C. Foudas, P. Gianneios, P. Katsoulis, P. Kokkas, S. Mallios, N. Manthos, I. Papadopoulos, E. Paradas, J. Strologas, F.A. Triantis, D. Tsitsonis

MTA-ELTE Lendület CMS Particle and Nuclear Physics Group, Eötvös Loránd University, Budapest, Hungary
M. Csanad, N. Filipovic, G. Pasztor, O. Surányi, G.I. Veres[20]

Wigner Research Centre for Physics, Budapest, Hungary
G. Bencze, C. Hajdu, D. Horvath[21], Á. Hunyadi, F. Sikler, V. Veszpremi, G. Vesztergombi[20]

Institute of Nuclear Research ATOMKI, Debrecen, Hungary
N. Beni, S. Czellar, J. Karancsi[22], A. Makovec, J. Molnar, Z. Szillasi

Institute of Physics, University of Debrecen, Debrecen, Hungary
M. Bartók[20], P. Raics, Z.L. Trocsanyi, B. Ujvari

Indian Institute of Science (IISc), Bangalore, India
S. Choudhury, J.R. Komaragiri

National Institute of Science Education and Research, Bhubaneswar, India
S. Bahinipati[23], P. Mal, K. Mandal, A. Nayak[24], D.K. Sahoo[23], N. Sahoo, S.K. Swain

Panjab University, Chandigarh, India
S. Bansal, S.B. Beri, V. Bhatnagar, R. Chawla, N. Dhingra, A. Kaur, M. Kaur, S. Kaur, R. Kumar, P. Kumari, A. Mehta, J.B. Singh, G. Walia

University of Delhi, Delhi, India
Ashok Kumar, Aashaq Shah, A. Bhardwaj, S. Chauhan, B.C. Choudhary, R.B. Garg, S. Keshri, A. Kumar, S. Malhotra, M. Naimuddin, K. Ranjan, R. Sharma

Saha Institute of Nuclear Physics, HBNI, Kolkata, India
R. Bhardwaj[25], R. Bhattacharya, S. Bhattacharya, U. Bhawandeep[25], D. Bhowmik, S. Dey, S. Dutt[25], S. Dutta, S. Ghosh, N. Majumdar, A. Modak, K. Mondal, S. Mukhopadhyay, S. Nandan, A. Purohit, P.K. Rout, A. Roy, S. Roy Chowdhury, S. Sarkar, M. Sharan, B. Singh, S. Thakur[25]

Indian Institute of Technology Madras, Madras, India
P.K. Behera

Bhabha Atomic Research Centre, Mumbai, India
R. Chudasama, D. Dutta, V. Jha, V. Kumar, A.K. Mohanty[16], P.K. Netrakanti, L.M. Pant, P. Shukla, A. Topkar

Tata Institute of Fundamental Research-A, Mumbai, India
T. Aziz, S. Dugad, B. Mahakud, S. Mitra, G.B. Mohanty, N. Sur, B. Sutar

Tata Institute of Fundamental Research-B, Mumbai, India
S. Banerjee, S. Bhattacharya, S. Chatterjee, P. Das, M. Guchait, Sa. Jain, S. Kumar, M. Maity[26], G. Majumder, K. Mazumdar, T. Sarkar[26], N. Wickramage[27]

Indian Institute of Science Education and Research (IISER), Pune, India
S. Chauhan, S. Dube, V. Hegde, A. Kapoor, K. Kothekar, S. Pandey, A. Rane, S. Sharma

Institute for Research in Fundamental Sciences (IPM), Tehran, Iran
S. Chenarani[28], E. Eskandari Tadavani, S.M. Etesami[28], M. Khakzad, M. Mohammadi Najafabadi, M. Naseri, S. Paktinat Mehdiabadi[29], F. Rezaei Hosseinabadi, B. Safarzadeh[30], M. Zeinali

University College Dublin, Dublin, Ireland
M. Felcini, M. Grunewald

INFN Sezione di Bari [a]**, Università di Bari** [b]**, Politecnico di Bari** [c]**, Bari, Italy**
M. Abbrescia[a,b], C. Calabria[a,b], A. Colaleo[a], D. Creanza[a,c], L. Cristella[a,b], N. De Filippis[a,c], M. De Palma[a,b], F. Errico[a,b], L. Fiore[a], G. Iaselli[a,c], S. Lezki[a,b], G. Maggi[a,c], M. Maggi[a], G. Miniello[a,b], S. My[a,b], S. Nuzzo[a,b], A. Pompili[a,b], G. Pugliese[a,c], R. Radogna[a], A. Ranieri[a], G. Selvaggi[a,b], A. Sharma[a], L. Silvestris[a,16], R. Venditti[a], P. Verwilligen[a]

INFN Sezione di Bologna [a]**, Università di Bologna** [b]**, Bologna, Italy**
G. Abbiendi[a], C. Battilana[a,b], D. Bonacorsi[a,b], L. Borgonovi[a,b], S. Braibant-Giacomelli[a,b], R. Campanini[a,b], P. Capiluppi[a,b], A. Castro[a,b], F.R. Cavallo[a], S.S. Chhibra[a,b], G. Codispoti[a,b], M. Cuffiani[a,b], G.M. Dallavalle[a], F. Fabbri[a], A. Fanfani[a,b], D. Fasanella[a,b], P. Giacomelli[a], C. Grandi[a], L. Guiducci[a,b], F. Iemmi, S. Marcellini[a], G. Masetti[a], A. Montanari[a], F.L. Navarria[a,b], A. Perrotta[a], A.M. Rossi[a,b], T. Rovelli[a,b], G.P. Siroli[a,b], N. Tosi[a]

INFN Sezione di Catania [a]**, Università di Catania** [b]**, Catania, Italy**
S. Albergo[a,b], S. Costa[a,b], A. Di Mattia[a], F. Giordano[a,b], R. Potenza[a,b], A. Tricomi[a,b], C. Tuve[a,b]

INFN Sezione di Firenze [a]**, Università di Firenze** [b]**, Firenze, Italy**
G. Barbagli[a], K. Chatterjee[a,b], V. Ciulli[a,b], C. Civinini[a], R. D'Alessandro[a,b], E. Focardi[a,b], P. Lenzi[a,b], M. Meschini[a], S. Paoletti[a], L. Russo[a,31], G. Sguazzoni[a], D. Strom[a], L. Viliani[a]

INFN Laboratori Nazionali di Frascati, Frascati, Italy
L. Benussi, S. Bianco, F. Fabbri, D. Piccolo, F. Primavera[16]

INFN Sezione di Genova [a]**, Università di Genova** [b]**, Genova, Italy**
V. Calvelli[a,b], F. Ferro[a], F. Ravera[a,b], E. Robutti[a], S. Tosi[a,b]

INFN Sezione di Milano-Bicocca [a]**, Università di Milano-Bicocca** [b]**, Milano, Italy**
A. Benaglia[a], A. Beschi[b], L. Brianza[a,b], F. Brivio[a,b], V. Ciriolo[a,b,16], M.E. Dinardo[a,b], S. Fiorendi[a,b], S. Gennai[a], A. Ghezzi[a,b], P. Govoni[a,b], M. Malberti[a,b], S. Malvezzi[a], R.A. Manzoni[a,b], D. Menasce[a], L. Moroni[a], M. Paganoni[a,b], K. Pauwels[a,b], D. Pedrini[a], S. Pigazzini[a,b,32], S. Ragazzi[a,b], T. Tabarelli de Fatis[a,b]

INFN Sezione di Napoli [a]**, Università di Napoli 'Federico II'** [b]**, Napoli, Italy, Università della Basilicata** [c]**, Potenza, Italy, Università G. Marconi** [d]**, Roma, Italy**
S. Buontempo[a], N. Cavallo[a,c], S. Di Guida[a,d,16], F. Fabozzi[a,c], F. Fienga[a,b], A.O.M. Iorio[a,b], W.A. Khan[a], L. Lista[a], S. Meola[a,d,16], P. Paolucci[a,16], C. Sciacca[a,b], F. Thyssen[a]

INFN Sezione di Padova [a]**, Università di Padova** [b]**, Padova, Italy, Università di Trento** [c]**, Trento, Italy**
P. Azzi[a], L. Benato[a,b], D. Bisello[a,b], A. Boletti[a,b], R. Carlin[a,b], A. Carvalho Antunes De Oliveira[a,b], P. Checchia[a], M. Dall'Osso[a,b], P. De Castro Manzano[a], T. Dorigo[a], U. Dosselli[a], F. Gasparini[a,b], U. Gasparini[a,b], A. Gozzelino[a], S. Lacaprara[a], P. Lujan, M. Margoni[a,b], A.T. Meneguzzo[a,b], N. Pozzobon[a,b], P. Ronchese[a,b], R. Rossin[a,b], F. Simonetto[a,b], A. Tiko, E. Torassa[a], S. Ventura[a], P. Zotto[a,b], G. Zumerle[a,b]

INFN Sezione di Pavia [a]**, Università di Pavia** [b]**, Pavia, Italy**
A. Braghieri[a], A. Magnani[a], P. Montagna[a,b], S.P. Ratti[a,b], V. Re[a], M. Ressegotti[a,b], C. Riccardi[a,b], P. Salvini[a], I. Vai[a,b], P. Vitulo[a,b]

INFN Sezione di Perugia [a]**, Università di Perugia** [b]**, Perugia, Italy**
L. Alunni Solestizi[a,b], M. Biasini[a,b], G.M. Bilei[a], C. Cecchi[a,b], D. Ciangottini[a,b], L. Fanò[a,b], P. Lariccia[a,b], R. Leonardi[a,b], E. Manoni[a], G. Mantovani[a,b], V. Mariani[a,b], M. Menichelli[a], A. Rossi[a,b], A. Santocchia[a,b], D. Spiga[a]

INFN Sezione di Pisa [a]**, Università di Pisa** [b]**, Scuola Normale Superiore di Pisa** [c]**, Pisa, Italy**
K. Androsov[a], P. Azzurri[a,16], G. Bagliesi[a], L. Bianchini[a], T. Boccali[a], L. Borrello, R. Castaldi[a], M.A. Ciocci[a,b], R. Dell'Orso[a], G. Fedi[a], L. Giannini[a,c], A. Giassi[a], M.T. Grippo[a,31], F. Ligabue[a,c], T. Lomtadze[a], E. Manca[a,c], G. Mandorli[a,c], A. Messineo[a,b], F. Palla[a], A. Rizzi[a,b], A. Savoy-Navarro[a,33], P. Spagnolo[a], R. Tenchini[a], G. Tonelli[a,b], A. Venturi[a], P.G. Verdini[a]

INFN Sezione di Roma [a]**, Sapienza Università di Roma** [b]**, Rome, Italy**
L. Barone[a,b], F. Cavallari[a], M. Cipriani[a,b], N. Daci[a], D. Del Re[a,b], E. Di Marco[a,b], M. Diemoz[a], S. Gelli[a,b], E. Longo[a,b], F. Margaroli[a,b], B. Marzocchi[a,b], P. Meridiani[a], G. Organtini[a,b], R. Paramatti[a,b], F. Preiato[a,b], S. Rahatlou[a,b], C. Rovelli[a], F. Santanastasio[a,b]

INFN Sezione di Torino [a]**, Università di Torino** [b]**, Torino, Italy, Università del Piemonte Orientale** [c]**, Novara, Italy**
N. Amapane[a,b], R. Arcidiacono[a,c], S. Argiro[a,b], M. Arneodo[a,c], N. Bartosik[a], R. Bellan[a,b],

C. Biino[a], N. Cartiglia[a], F. Cenna[a,b], M. Costa[a,b], R. Covarelli[a,b], A. Degano[a,b], N. Demaria[a], B. Kiani[a,b], C. Mariotti[a], S. Maselli[a], E. Migliore[a,b], V. Monaco[a,b], E. Monteil[a,b], M. Monteno[a], M.M. Obertino[a,b], L. Pacher[a,b], N. Pastrone[a], M. Pelliccioni[a], G.L. Pinna Angioni[a,b], A. Romero[a,b], M. Ruspa[a,c], R. Sacchi[a,b], K. Shchelina[a,b], V. Sola[a], A. Solano[a,b], A. Staiano[a], P. Traczyk[a,b]

INFN Sezione di Trieste [a], Università di Trieste [b], Trieste, Italy
S. Belforte[a], M. Casarsa[a], F. Cossutti[a], G. Della Ricca[a,b], A. Zanetti[a]

Kyungpook National University, Daegu, Korea
D.H. Kim, G.N. Kim, M.S. Kim, J. Lee, S. Lee, S.W. Lee, C.S. Moon, Y.D. Oh, S. Sekmen, D.C. Son, Y.C. Yang

Chonnam National University, Institute for Universe and Elementary Particles, Kwangju, Korea
H. Kim, D.H. Moon, G. Oh

Hanyang University, Seoul, Korea
J.A. Brochero Cifuentes, J. Goh, T.J. Kim

Korea University, Seoul, Korea
S. Cho, S. Choi, Y. Go, D. Gyun, S. Ha, B. Hong, Y. Jo, Y. Kim, K. Lee, K.S. Lee, S. Lee, J. Lim, S.K. Park, Y. Roh

Seoul National University, Seoul, Korea
J. Almond, J. Kim, J.S. Kim, H. Lee, K. Lee, K. Nam, S.B. Oh, B.C. Radburn-Smith, S.h. Seo, U.K. Yang, H.D. Yoo, G.B. Yu

University of Seoul, Seoul, Korea
H. Kim, J.H. Kim, J.S.H. Lee, I.C. Park

Sungkyunkwan University, Suwon, Korea
Y. Choi, C. Hwang, J. Lee, I. Yu

Vilnius University, Vilnius, Lithuania
V. Dudenas, A. Juodagalvis, J. Vaitkus

National Centre for Particle Physics, Universiti Malaya, Kuala Lumpur, Malaysia
I. Ahmed, Z.A. Ibrahim, M.A.B. Md Ali[34], F. Mohamad Idris[35], W.A.T. Wan Abdullah, M.N. Yusli, Z. Zolkapli

Centro de Investigacion y de Estudios Avanzados del IPN, Mexico City, Mexico
Reyes-Almanza, R, Ramirez-Sanchez, G., Duran-Osuna, M. C., H. Castilla-Valdez, E. De La Cruz-Burelo, I. Heredia-De La Cruz[36], Rabadan-Trejo, R. I., R. Lopez-Fernandez, J. Mejia Guisao, A. Sanchez-Hernandez

Universidad Iberoamericana, Mexico City, Mexico
S. Carrillo Moreno, C. Oropeza Barrera, F. Vazquez Valencia

Benemerita Universidad Autonoma de Puebla, Puebla, Mexico
J. Eysermans, I. Pedraza, H.A. Salazar Ibarguen, C. Uribe Estrada

Universidad Autónoma de San Luis Potosí, San Luis Potosí, Mexico
A. Morelos Pineda

University of Auckland, Auckland, New Zealand
D. Krofcheck

University of Canterbury, Christchurch, New Zealand
P.H. Butler

National Centre for Physics, Quaid-I-Azam University, Islamabad, Pakistan
A. Ahmad, M. Ahmad, Q. Hassan, H.R. Hoorani, A. Saddique, M.A. Shah, M. Shoaib, M. Waqas

National Centre for Nuclear Research, Swierk, Poland
H. Bialkowska, M. Bluj, B. Boimska, T. Frueboes, M. Górski, M. Kazana, K. Nawrocki, M. Szleper, P. Zalewski

Institute of Experimental Physics, Faculty of Physics, University of Warsaw, Warsaw, Poland
K. Bunkowski, A. Byszuk[37], K. Doroba, A. Kalinowski, M. Konecki, J. Krolikowski, M. Misiura, M. Olszewski, A. Pyskir, M. Walczak

Laboratório de Instrumentação e Física Experimental de Partículas, Lisboa, Portugal
P. Bargassa, C. Beirão Da Cruz E Silva, A. Di Francesco, P. Faccioli, B. Galinhas, M. Gallinaro, J. Hollar, N. Leonardo, L. Lloret Iglesias, M.V. Nemallapudi, J. Seixas, G. Strong, O. Toldaiev, D. Vadruccio, J. Varela

Joint Institute for Nuclear Research, Dubna, Russia
S. Afanasiev, P. Bunin, M. Gavrilenko, I. Golutvin, I. Gorbunov, A. Kamenev, V. Karjavin, A. Lanev, A. Malakhov, V. Matveev[38,39], P. Moisenz, V. Palichik, V. Perelygin, S. Shmatov, S. Shulha, N. Skatchkov, V. Smirnov, N. Voytishin, A. Zarubin

Petersburg Nuclear Physics Institute, Gatchina (St. Petersburg), Russia
Y. Ivanov, V. Kim[40], E. Kuznetsova[41], P. Levchenko, V. Murzin, V. Oreshkin, I. Smirnov, D. Sosnov, V. Sulimov, L. Uvarov, S. Vavilov, A. Vorobyev

Institute for Nuclear Research, Moscow, Russia
Yu. Andreev, A. Dermenev, S. Gninenko, N. Golubev, A. Karneyeu, M. Kirsanov, N. Krasnikov, A. Pashenkov, D. Tlisov, A. Toropin

Institute for Theoretical and Experimental Physics, Moscow, Russia
V. Epshteyn, V. Gavrilov, N. Lychkovskaya, V. Popov, I. Pozdnyakov, G. Safronov, A. Spiridonov, A. Stepennov, V. Stolin, M. Toms, E. Vlasov, A. Zhokin

Moscow Institute of Physics and Technology, Moscow, Russia
T. Aushev, A. Bylinkin[39]

National Research Nuclear University 'Moscow Engineering Physics Institute' (MEPhI), Moscow, Russia
M. Chadeeva[42], P. Parygin, D. Philippov, S. Polikarpov, E. Popova, V. Rusinov

P.N. Lebedev Physical Institute, Moscow, Russia
V. Andreev, M. Azarkin[39], I. Dremin[39], M. Kirakosyan[39], S.V. Rusakov, A. Terkulov

Skobeltsyn Institute of Nuclear Physics, Lomonosov Moscow State University, Moscow, Russia
A. Baskakov, A. Belyaev, E. Boos, V. Bunichev, M. Dubinin[43], L. Dudko, A. Gribushin, V. Klyukhin, N. Korneeva, I. Lokhtin, I. Miagkov, S. Obraztsov, M. Perfilov, V. Savrin, P. Volkov

Novosibirsk State University (NSU), Novosibirsk, Russia
V. Blinov[44], D. Shtol[44], Y. Skovpen[44]

State Research Center of Russian Federation, Institute for High Energy Physics of NRC "Kurchatov Institute", Protvino, Russia
I. Azhgirey, I. Bayshev, S. Bitioukov, D. Elumakhov, A. Godizov, V. Kachanov, A. Kalinin, D. Konstantinov, P. Mandrik, V. Petrov, R. Ryutin, A. Sobol, S. Troshin, N. Tyurin, A. Uzunian, A. Volkov

University of Belgrade, Faculty of Physics and Vinca Institute of Nuclear Sciences, Belgrade, Serbia
P. Adzic[45], P. Cirkovic, D. Devetak, M. Dordevic, J. Milosevic

Centro de Investigaciones Energéticas Medioambientales y Tecnológicas (CIEMAT), Madrid, Spain
J. Alcaraz Maestre, I. Bachiller, M. Barrio Luna, M. Cerrada, N. Colino, B. De La Cruz, A. Delgado Peris, C. Fernandez Bedoya, J.P. Fernández Ramos, J. Flix, M.C. Fouz, O. Gonzalez Lopez, S. Goy Lopez, J.M. Hernandez, M.I. Josa, D. Moran, A. Pérez-Calero Yzquierdo, J. Puerta Pelayo, I. Redondo, L. Romero, M.S. Soares, A. Triossi, A. Álvarez Fernández

Universidad Autónoma de Madrid, Madrid, Spain
C. Albajar, J.F. de Trocóniz

Universidad de Oviedo, Oviedo, Spain
J. Cuevas, C. Erice, J. Fernandez Menendez, I. Gonzalez Caballero, J.R. González Fernández, E. Palencia Cortezon, S. Sanchez Cruz, P. Vischia, J.M. Vizan Garcia

Instituto de Física de Cantabria (IFCA), CSIC-Universidad de Cantabria, Santander, Spain
I.J. Cabrillo, A. Calderon, B. Chazin Quero, E. Curras, J. Duarte Campderros, M. Fernandez, P.J. Fernández Manteca, J. Garcia-Ferrero, A. García Alonso, G. Gomez, A. Lopez Virto, J. Marco, C. Martinez Rivero, P. Martinez Ruiz del Arbol, F. Matorras, J. Piedra Gomez, C. Prieels, T. Rodrigo, A. Ruiz-Jimeno, L. Scodellaro, N. Trevisani, I. Vila, R. Vilar Cortabitarte

CERN, European Organization for Nuclear Research, Geneva, Switzerland
D. Abbaneo, B. Akgun, E. Auffray, P. Baillon, A.H. Ball, D. Barney, J. Bendavid, M. Bianco, A. Bocci, C. Botta, T. Camporesi, R. Castello, M. Cepeda, G. Cerminara, E. Chapon, Y. Chen, D. d'Enterria, A. Dabrowski, V. Daponte, A. David, M. De Gruttola, A. De Roeck, N. Deelen, M. Dobson, T. du Pree, M. Dünser, N. Dupont, A. Elliott-Peisert, P. Everaerts, F. Fallavollita, G. Franzoni, J. Fulcher, W. Funk, D. Gigi, A. Gilbert, K. Gill, F. Glege, D. Gulhan, J. Hegeman, V. Innocente, A. Jafari, P. Janot, O. Karacheban[19], J. Kieseler, V. Knünz, A. Kornmayer, M.J. Kortelainen, M. Krammer[1], C. Lange, P. Lecoq, C. Lourenço, M.T. Lucchini, L. Malgeri, M. Mannelli, A. Martelli, F. Meijers, J.A. Merlin, S. Mersi, E. Meschi, P. Milenovic[46], F. Moortgat, M. Mulders, H. Neugebauer, J. Ngadiuba, S. Orfanelli, L. Orsini, L. Pape, E. Perez, M. Peruzzi, A. Petrilli, G. Petrucciani, A. Pfeiffer, M. Pierini, F.M. Pitters, D. Rabady, A. Racz, T. Reis, G. Rolandi[47], M. Rovere, H. Sakulin, C. Schäfer, C. Schwick, M. Seidel, M. Selvaggi, A. Sharma, P. Silva, P. Sphicas[48], A. Stakia, J. Steggemann, M. Stoye, M. Tosi, D. Treille, A. Tsirou, V. Veckalns[49], M. Verweij, W.D. Zeuner

Paul Scherrer Institut, Villigen, Switzerland
W. Bertl[†], L. Caminada[50], K. Deiters, W. Erdmann, R. Horisberger, Q. Ingram, H.C. Kaestli, D. Kotlinski, U. Langenegger, T. Rohe, S.A. Wiederkehr

ETH Zurich - Institute for Particle Physics and Astrophysics (IPA), Zurich, Switzerland
M. Backhaus, L. Bäni, P. Berger, B. Casal, G. Dissertori, M. Dittmar, M. Donegà, C. Dorfer, C. Grab, C. Heidegger, D. Hits, J. Hoss, G. Kasieczka, T. Klijnsma, W. Lustermann, B. Mangano, M. Marionneau, M.T. Meinhard, D. Meister, F. Micheli, P. Musella, F. Nessi-Tedaldi, F. Pandolfi,

J. Pata, F. Pauss, G. Perrin, L. Perrozzi, M. Quittnat, M. Reichmann, D.A. Sanz Becerra, M. Schönenberger, L. Shchutska, V.R. Tavolaro, K. Theofilatos, M.L. Vesterbacka Olsson, R. Wallny, D.H. Zhu

Universität Zürich, Zurich, Switzerland
T.K. Aarrestad, C. Amsler[51], M.F. Canelli, A. De Cosa, R. Del Burgo, S. Donato, C. Galloni, T. Hreus, B. Kilminster, D. Pinna, G. Rauco, P. Robmann, D. Salerno, K. Schweiger, C. Seitz, Y. Takahashi, A. Zucchetta

National Central University, Chung-Li, Taiwan
V. Candelise, Y.H. Chang, K.y. Cheng, T.H. Doan, Sh. Jain, R. Khurana, C.M. Kuo, W. Lin, A. Pozdnyakov, S.S. Yu

National Taiwan University (NTU), Taipei, Taiwan
Arun Kumar, P. Chang, Y. Chao, K.F. Chen, P.H. Chen, F. Fiori, W.-S. Hou, Y. Hsiung, Y.F. Liu, R.-S. Lu, E. Paganis, A. Psallidas, A. Steen, J.f. Tsai

Chulalongkorn University, Faculty of Science, Department of Physics, Bangkok, Thailand
B. Asavapibhop, K. Kovitanggoon, G. Singh, N. Srimanobhas

Çukurova University, Physics Department, Science and Art Faculty, Adana, Turkey
A. Bat, F. Boran, S. Cerci[52], S. Damarseckin, Z.S. Demiroglu, C. Dozen, I. Dumanoglu, S. Girgis, G. Gokbulut, Y. Guler, I. Hos[53], E.E. Kangal[54], O. Kara, A. Kayis Topaksu, U. Kiminsu, M. Oglakci, G. Onengut, K. Ozdemir[55], D. Sunar Cerci[52], B. Tali[52], U.G. Tok, S. Turkcapar, I.S. Zorbakir, C. Zorbilmez

Middle East Technical University, Physics Department, Ankara, Turkey
G. Karapinar[56], K. Ocalan[57], M. Yalvac, M. Zeyrek

Bogazici University, Istanbul, Turkey
E. Gülmez, M. Kaya[58], O. Kaya[59], S. Tekten, E.A. Yetkin[60]

Istanbul Technical University, Istanbul, Turkey
M.N. Agaras, S. Atay, A. Cakir, K. Cankocak, Y. Komurcu

Institute for Scintillation Materials of National Academy of Science of Ukraine, Kharkov, Ukraine
B. Grynyov

National Scientific Center, Kharkov Institute of Physics and Technology, Kharkov, Ukraine
L. Levchuk

University of Bristol, Bristol, United Kingdom
F. Ball, L. Beck, J.J. Brooke, D. Burns, E. Clement, D. Cussans, O. Davignon, H. Flacher, J. Goldstein, G.P. Heath, H.F. Heath, L. Kreczko, D.M. Newbold[61], S. Paramesvaran, T. Sakuma, S. Seif El Nasr-storey, D. Smith, V.J. Smith

Rutherford Appleton Laboratory, Didcot, United Kingdom
K.W. Bell, A. Belyaev[62], C. Brew, R.M. Brown, L. Calligaris, D. Cieri, D.J.A. Cockerill, J.A. Coughlan, K. Harder, S. Harper, J. Linacre, E. Olaiya, D. Petyt, C.H. Shepherd-Themistocleous, A. Thea, I.R. Tomalin, T. Williams, W.J. Womersley

Imperial College, London, United Kingdom
G. Auzinger, R. Bainbridge, P. Bloch, J. Borg, S. Breeze, O. Buchmuller, A. Bundock, S. Casasso, M. Citron, D. Colling, L. Corpe, P. Dauncey, G. Davies, M. Della Negra, R. Di Maria, Y. Haddad, G. Hall, G. Iles, T. James, R. Lane, C. Laner, L. Lyons, A.-M. Magnan, S. Malik, L. Mastrolorenzo,

T. Matsushita, J. Nash[63], A. Nikitenko[6], V. Palladino, M. Pesaresi, D.M. Raymond, A. Richards, A. Rose, E. Scott, C. Seez, A. Shtipliyski, S. Summers, A. Tapper, K. Uchida, M. Vazquez Acosta[64], T. Virdee[16], N. Wardle, D. Winterbottom, J. Wright, S.C. Zenz

Brunel University, Uxbridge, United Kingdom
J.E. Cole, P.R. Hobson, A. Khan, P. Kyberd, A. Morton, I.D. Reid, L. Teodorescu, S. Zahid

Baylor University, Waco, USA
A. Borzou, K. Call, J. Dittmann, K. Hatakeyama, H. Liu, N. Pastika, C. Smith

Catholic University of America, Washington DC, USA
R. Bartek, A. Dominguez

The University of Alabama, Tuscaloosa, USA
A. Buccilli, S.I. Cooper, C. Henderson, P. Rumerio, C. West

Boston University, Boston, USA
D. Arcaro, A. Avetisyan, T. Bose, D. Gastler, D. Rankin, C. Richardson, J. Rohlf, L. Sulak, D. Zou

Brown University, Providence, USA
G. Benelli, D. Cutts, M. Hadley, J. Hakala, U. Heintz, J.M. Hogan, K.H.M. Kwok, E. Laird, G. Landsberg, J. Lee, Z. Mao, M. Narain, J. Pazzini, S. Piperov, S. Sagir, R. Syarif, D. Yu

University of California, Davis, Davis, USA
R. Band, C. Brainerd, R. Breedon, D. Burns, M. Calderon De La Barca Sanchez, M. Chertok, J. Conway, R. Conway, P.T. Cox, R. Erbacher, C. Flores, G. Funk, W. Ko, R. Lander, C. Mclean, M. Mulhearn, D. Pellett, J. Pilot, S. Shalhout, M. Shi, J. Smith, D. Stolp, D. Taylor, K. Tos, M. Tripathi, Z. Wang

University of California, Los Angeles, USA
M. Bachtis, C. Bravo, R. Cousins, A. Dasgupta, A. Florent, J. Hauser, M. Ignatenko, N. Mccoll, S. Regnard, D. Saltzberg, C. Schnaible, V. Valuev

University of California, Riverside, Riverside, USA
E. Bouvier, K. Burt, R. Clare, J. Ellison, J.W. Gary, S.M.A. Ghiasi Shirazi, G. Hanson, J. Heilman, G. Karapostoli, E. Kennedy, F. Lacroix, O.R. Long, M. Olmedo Negrete, M.I. Paneva, W. Si, L. Wang, H. Wei, S. Wimpenny, B. R. Yates

University of California, San Diego, La Jolla, USA
J.G. Branson, S. Cittolin, M. Derdzinski, R. Gerosa, D. Gilbert, B. Hashemi, A. Holzner, D. Klein, G. Kole, V. Krutelyov, J. Letts, M. Masciovecchio, D. Olivito, S. Padhi, M. Pieri, M. Sani, V. Sharma, S. Simon, M. Tadel, A. Vartak, S. Wasserbaech[65], J. Wood, F. Würthwein, A. Yagil, G. Zevi Della Porta

University of California, Santa Barbara - Department of Physics, Santa Barbara, USA
N. Amin, R. Bhandari, J. Bradmiller-Feld, C. Campagnari, A. Dishaw, V. Dutta, M. Franco Sevilla, L. Gouskos, R. Heller, J. Incandela, A. Ovcharova, H. Qu, J. Richman, D. Stuart, I. Suarez, J. Yoo

California Institute of Technology, Pasadena, USA
D. Anderson, A. Bornheim, J. Bunn, I. Dutta, J.M. Lawhorn, H.B. Newman, T. Q. Nguyen, C. Pena, M. Spiropulu, J.R. Vlimant, R. Wilkinson, S. Xie, Z. Zhang, R.Y. Zhu

Carnegie Mellon University, Pittsburgh, USA
M.B. Andrews, T. Ferguson, T. Mudholkar, M. Paulini, J. Russ, M. Sun, H. Vogel, I. Vorobiev, M. Weinberg

University of Colorado Boulder, Boulder, USA
J.P. Cumalat, W.T. Ford, F. Jensen, A. Johnson, M. Krohn, S. Leontsinis, E. Macdonald, T. Mulholland, K. Stenson, S.R. Wagner

Cornell University, Ithaca, USA
J. Alexander, J. Chaves, Y. Cheng, J. Chu, S. Dittmer, K. Mcdermott, N. Mirman, J.R. Patterson, D. Quach, A. Rinkevicius, A. Ryd, L. Skinnari, L. Soffi, S.M. Tan, Z. Tao, J. Thom, J. Tucker, P. Wittich, M. Zientek

Fermi National Accelerator Laboratory, Batavia, USA
S. Abdullin, M. Albrow, M. Alyari, G. Apollinari, A. Apresyan, A. Apyan, S. Banerjee, L.A.T. Bauerdick, A. Beretvas, J. Berryhill, P.C. Bhat, G. Bolla[†], K. Burkett, J.N. Butler, A. Canepa, G.B. Cerati, H.W.K. Cheung, F. Chlebana, M. Cremonesi, J. Duarte, V.D. Elvira, J. Freeman, Z. Gecse, E. Gottschalk, L. Gray, D. Green, S. Grünendahl, O. Gutsche, J. Hanlon, R.M. Harris, S. Hasegawa, J. Hirschauer, Z. Hu, B. Jayatilaka, S. Jindariani, M. Johnson, U. Joshi, B. Klima, B. Kreis, S. Lammel, D. Lincoln, R. Lipton, M. Liu, T. Liu, R. Lopes De Sá, J. Lykken, K. Maeshima, N. Magini, J.M. Marraffino, D. Mason, P. McBride, P. Merkel, S. Mrenna, S. Nahn, V. O'Dell, K. Pedro, O. Prokofyev, G. Rakness, L. Ristori, B. Schneider, E. Sexton-Kennedy, A. Soha, W.J. Spalding, L. Spiegel, S. Stoynev, J. Strait, N. Strobbe, L. Taylor, S. Tkaczyk, N.V. Tran, L. Uplegger, E.W. Vaandering, C. Vernieri, M. Verzocchi, R. Vidal, M. Wang, H.A. Weber, A. Whitbeck, W. Wu

University of Florida, Gainesville, USA
D. Acosta, P. Avery, P. Bortignon, D. Bourilkov, A. Brinkerhoff, A. Carnes, M. Carver, D. Curry, R.D. Field, I.K. Furic, S.V. Gleyzer, B.M. Joshi, J. Konigsberg, A. Korytov, K. Kotov, P. Ma, K. Matchev, H. Mei, G. Mitselmakher, K. Shi, D. Sperka, N. Terentyev, L. Thomas, J. Wang, S. Wang, J. Yelton

Florida International University, Miami, USA
Y.R. Joshi, S. Linn, P. Markowitz, J.L. Rodriguez

Florida State University, Tallahassee, USA
A. Ackert, T. Adams, A. Askew, S. Hagopian, V. Hagopian, K.F. Johnson, T. Kolberg, G. Martinez, T. Perry, H. Prosper, A. Saha, A. Santra, V. Sharma, R. Yohay

Florida Institute of Technology, Melbourne, USA
M.M. Baarmand, V. Bhopatkar, S. Colafranceschi, M. Hohlmann, D. Noonan, T. Roy, F. Yumiceva

University of Illinois at Chicago (UIC), Chicago, USA
M.R. Adams, L. Apanasevich, D. Berry, R.R. Betts, R. Cavanaugh, X. Chen, O. Evdokimov, C.E. Gerber, D.A. Hangal, D.J. Hofman, K. Jung, J. Kamin, I.D. Sandoval Gonzalez, M.B. Tonjes, H. Trauger, N. Varelas, H. Wang, Z. Wu, J. Zhang

The University of Iowa, Iowa City, USA
B. Bilki[66], W. Clarida, K. Dilsiz[67], S. Durgut, R.P. Gandrajula, M. Haytmyradov, V. Khristenko, J.-P. Merlo, H. Mermerkaya[68], A. Mestvirishvili, A. Moeller, J. Nachtman, H. Ogul[69], Y. Onel, F. Ozok[70], A. Penzo, C. Snyder, E. Tiras, J. Wetzel, K. Yi

Johns Hopkins University, Baltimore, USA
B. Blumenfeld, A. Cocoros, N. Eminizer, D. Fehling, L. Feng, A.V. Gritsan, P. Maksimovic, J. Roskes, U. Sarica, M. Swartz, M. Xiao, C. You

The University of Kansas, Lawrence, USA
A. Al-bataineh, P. Baringer, A. Bean, S. Boren, J. Bowen, J. Castle, S. Khalil, A. Kropivnitskaya, D. Majumder, W. Mcbrayer, M. Murray, C. Rogan, C. Royon, S. Sanders, E. Schmitz, J.D. Tapia Takaki, Q. Wang

Kansas State University, Manhattan, USA
A. Ivanov, K. Kaadze, Y. Maravin, A. Mohammadi, L.K. Saini, N. Skhirtladze

Lawrence Livermore National Laboratory, Livermore, USA
F. Rebassoo, D. Wright

University of Maryland, College Park, USA
A. Baden, O. Baron, A. Belloni, S.C. Eno, Y. Feng, C. Ferraioli, N.J. Hadley, S. Jabeen, G.Y. Jeng, R.G. Kellogg, J. Kunkle, A.C. Mignerey, F. Ricci-Tam, Y.H. Shin, A. Skuja, S.C. Tonwar

Massachusetts Institute of Technology, Cambridge, USA
D. Abercrombie, B. Allen, V. Azzolini, R. Barbieri, A. Baty, G. Bauer, R. Bi, S. Brandt, W. Busza, I.A. Cali, M. D'Alfonso, Z. Demiragli, G. Gomez Ceballos, M. Goncharov, P. Harris, D. Hsu, M. Hu, Y. Iiyama, G.M. Innocenti, M. Klute, D. Kovalskyi, Y.-J. Lee, A. Levin, P.D. Luckey, B. Maier, A.C. Marini, C. Mcginn, C. Mironov, S. Narayanan, X. Niu, C. Paus, C. Roland, G. Roland, J. Salfeld-Nebgen, G.S.F. Stephans, K. Sumorok, K. Tatar, D. Velicanu, J. Wang, T.W. Wang, B. Wyslouch

University of Minnesota, Minneapolis, USA
A.C. Benvenuti, R.M. Chatterjee, A. Evans, P. Hansen, J. Hiltbrand, S. Kalafut, Y. Kubota, Z. Lesko, J. Mans, S. Nourbakhsh, N. Ruckstuhl, R. Rusack, J. Turkewitz, M.A. Wadud

University of Mississippi, Oxford, USA
J.G. Acosta, S. Oliveros

University of Nebraska-Lincoln, Lincoln, USA
E. Avdeeva, K. Bloom, D.R. Claes, C. Fangmeier, F. Golf, R. Gonzalez Suarez, R. Kamalieddin, I. Kravchenko, J. Monroy, J.E. Siado, G.R. Snow, B. Stieger

State University of New York at Buffalo, Buffalo, USA
J. Dolen, A. Godshalk, C. Harrington, I. Iashvili, D. Nguyen, A. Parker, S. Rappoccio, B. Roozbahani

Northeastern University, Boston, USA
G. Alverson, E. Barberis, C. Freer, A. Hortiangtham, A. Massironi, D.M. Morse, T. Orimoto, R. Teixeira De Lima, T. Wamorkar, B. Wang, A. Wisecarver, D. Wood

Northwestern University, Evanston, USA
S. Bhattacharya, O. Charaf, K.A. Hahn, N. Mucia, N. Odell, M.H. Schmitt, K. Sung, M. Trovato, M. Velasco

University of Notre Dame, Notre Dame, USA
R. Bucci, N. Dev, M. Hildreth, K. Hurtado Anampa, C. Jessop, D.J. Karmgard, N. Kellams, K. Lannon, W. Li, N. Loukas, N. Marinelli, F. Meng, C. Mueller, Y. Musienko[38], M. Planer, A. Reinsvold, R. Ruchti, P. Siddireddy, G. Smith, S. Taroni, M. Wayne, A. Wightman, M. Wolf, A. Woodard

The Ohio State University, Columbus, USA
J. Alimena, L. Antonelli, B. Bylsma, L.S. Durkin, S. Flowers, B. Francis, A. Hart, C. Hill, W. Ji, T.Y. Ling, B. Liu, W. Luo, B.L. Winer, H.W. Wulsin

Princeton University, Princeton, USA
S. Cooperstein, O. Driga, P. Elmer, J. Hardenbrook, P. Hebda, S. Higginbotham, A. Kalogeropoulos, D. Lange, J. Luo, D. Marlow, K. Mei, I. Ojalvo, J. Olsen, C. Palmer, P. Piroué, D. Stickland, C. Tully

University of Puerto Rico, Mayaguez, USA
S. Malik, S. Norberg

Purdue University, West Lafayette, USA
A. Barker, V.E. Barnes, S. Das, S. Folgueras, L. Gutay, M. Jones, A.W. Jung, A. Khatiwada, D.H. Miller, N. Neumeister, C.C. Peng, H. Qiu, J.F. Schulte, J. Sun, F. Wang, R. Xiao, W. Xie

Purdue University Northwest, Hammond, USA
T. Cheng, N. Parashar, J. Stupak

Rice University, Houston, USA
Z. Chen, K.M. Ecklund, S. Freed, F.J.M. Geurts, M. Guilbaud, M. Kilpatrick, W. Li, B. Michlin, B.P. Padley, J. Roberts, J. Rorie, W. Shi, Z. Tu, J. Zabel, A. Zhang

University of Rochester, Rochester, USA
A. Bodek, P. de Barbaro, R. Demina, Y.t. Duh, T. Ferbel, M. Galanti, A. Garcia-Bellido, J. Han, O. Hindrichs, A. Khukhunaishvili, K.H. Lo, P. Tan, M. Verzetti

The Rockefeller University, New York, USA
R. Ciesielski, K. Goulianos, C. Mesropian

Rutgers, The State University of New Jersey, Piscataway, USA
A. Agapitos, J.P. Chou, Y. Gershtein, T.A. Gómez Espinosa, E. Halkiadakis, M. Heindl, E. Hughes, S. Kaplan, R. Kunnawalkam Elayavalli, S. Kyriacou, A. Lath, R. Montalvo, K. Nash, M. Osherson, H. Saka, S. Salur, S. Schnetzer, D. Sheffield, S. Somalwar, R. Stone, S. Thomas, P. Thomassen, M. Walker

University of Tennessee, Knoxville, USA
A.G. Delannoy, J. Heideman, G. Riley, K. Rose, S. Spanier, K. Thapa

Texas A&M University, College Station, USA
O. Bouhali[71], A. Castaneda Hernandez[71], A. Celik, M. Dalchenko, M. De Mattia, A. Delgado, S. Dildick, R. Eusebi, J. Gilmore, T. Huang, T. Kamon[72], R. Mueller, Y. Pakhotin, R. Patel, A. Perloff, L. Perniè, D. Rathjens, A. Safonov, A. Tatarinov, K.A. Ulmer

Texas Tech University, Lubbock, USA
N. Akchurin, J. Damgov, F. De Guio, P.R. Dudero, J. Faulkner, E. Gurpinar, S. Kunori, K. Lamichhane, S.W. Lee, T. Mengke, S. Muthumuni, T. Peltola, S. Undleeb, I. Volobouev, Z. Wang

Vanderbilt University, Nashville, USA
S. Greene, A. Gurrola, R. Janjam, W. Johns, C. Maguire, A. Melo, H. Ni, K. Padeken, P. Sheldon, S. Tuo, J. Velkovska, Q. Xu

University of Virginia, Charlottesville, USA
M.W. Arenton, P. Barria, B. Cox, R. Hirosky, M. Joyce, A. Ledovskoy, H. Li, C. Neu, T. Sinthuprasith, Y. Wang, E. Wolfe, F. Xia

Wayne State University, Detroit, USA
R. Harr, P.E. Karchin, N. Poudyal, J. Sturdy, P. Thapa, S. Zaleski

University of Wisconsin - Madison, Madison, WI, USA

M. Brodski, J. Buchanan, C. Caillol, D. Carlsmith, S. Dasu, L. Dodd, S. Duric, B. Gomber, M. Grothe, M. Herndon, A. Hervé, U. Hussain, P. Klabbers, A. Lanaro, A. Levine, K. Long, R. Loveless, V. Rekovic, T. Ruggles, A. Savin, N. Smith, W.H. Smith, N. Woods

†: Deceased

1: Also at Vienna University of Technology, Vienna, Austria

2: Also at IRFU, CEA, Université Paris-Saclay, Gif-sur-Yvette, France

3: Also at Universidade Estadual de Campinas, Campinas, Brazil

4: Also at Federal University of Rio Grande do Sul, Porto Alegre, Brazil

5: Also at Université Libre de Bruxelles, Bruxelles, Belgium

6: Also at Institute for Theoretical and Experimental Physics, Moscow, Russia

7: Also at Joint Institute for Nuclear Research, Dubna, Russia

8: Also at Suez University, Suez, Egypt

9: Now at British University in Egypt, Cairo, Egypt

10: Also at Fayoum University, El-Fayoum, Egypt

11: Now at Helwan University, Cairo, Egypt

12: Also at Department of Physics, King Abdulaziz University, Jeddah, Saudi Arabia

13: Also at Université de Haute Alsace, Mulhouse, France

14: Also at Skobeltsyn Institute of Nuclear Physics, Lomonosov Moscow State University, Moscow, Russia

15: Also at Tbilisi State University, Tbilisi, Georgia

16: Also at CERN, European Organization for Nuclear Research, Geneva, Switzerland

17: Also at RWTH Aachen University, III. Physikalisches Institut A, Aachen, Germany

18: Also at University of Hamburg, Hamburg, Germany

19: Also at Brandenburg University of Technology, Cottbus, Germany

20: Also at MTA-ELTE Lendület CMS Particle and Nuclear Physics Group, Eötvös Loránd University, Budapest, Hungary

21: Also at Institute of Nuclear Research ATOMKI, Debrecen, Hungary

22: Also at Institute of Physics, University of Debrecen, Debrecen, Hungary

23: Also at Indian Institute of Technology Bhubaneswar, Bhubaneswar, India

24: Also at Institute of Physics, Bhubaneswar, India

25: Also at Shoolini University, Solan, India

26: Also at University of Visva-Bharati, Santiniketan, India

27: Also at University of Ruhuna, Matara, Sri Lanka

28: Also at Isfahan University of Technology, Isfahan, Iran

29: Also at Yazd University, Yazd, Iran

30: Also at Plasma Physics Research Center, Science and Research Branch, Islamic Azad University, Tehran, Iran

31: Also at Università degli Studi di Siena, Siena, Italy

32: Also at INFN Sezione di Milano-Bicocca; Università di Milano-Bicocca, Milano, Italy

33: Also at Purdue University, West Lafayette, USA

34: Also at International Islamic University of Malaysia, Kuala Lumpur, Malaysia

35: Also at Malaysian Nuclear Agency, MOSTI, Kajang, Malaysia

36: Also at Consejo Nacional de Ciencia y Tecnología, Mexico city, Mexico

37: Also at Warsaw University of Technology, Institute of Electronic Systems, Warsaw, Poland

38: Also at Institute for Nuclear Research, Moscow, Russia

39: Now at National Research Nuclear University 'Moscow Engineering Physics Institute' (MEPhI), Moscow, Russia

40: Also at St. Petersburg State Polytechnical University, St. Petersburg, Russia

41: Also at University of Florida, Gainesville, USA
42: Also at P.N. Lebedev Physical Institute, Moscow, Russia
43: Also at California Institute of Technology, Pasadena, USA
44: Also at Budker Institute of Nuclear Physics, Novosibirsk, Russia
45: Also at Faculty of Physics, University of Belgrade, Belgrade, Serbia
46: Also at University of Belgrade, Faculty of Physics and Vinca Institute of Nuclear Sciences, Belgrade, Serbia
47: Also at Scuola Normale e Sezione dell'INFN, Pisa, Italy
48: Also at National and Kapodistrian University of Athens, Athens, Greece
49: Also at Riga Technical University, Riga, Latvia
50: Also at Universität Zürich, Zurich, Switzerland
51: Also at Stefan Meyer Institute for Subatomic Physics (SMI), Vienna, Austria
52: Also at Adiyaman University, Adiyaman, Turkey
53: Also at Istanbul Aydin University, Istanbul, Turkey
54: Also at Mersin University, Mersin, Turkey
55: Also at Piri Reis University, Istanbul, Turkey
56: Also at Izmir Institute of Technology, Izmir, Turkey
57: Also at Necmettin Erbakan University, Konya, Turkey
58: Also at Marmara University, Istanbul, Turkey
59: Also at Kafkas University, Kars, Turkey
60: Also at Istanbul Bilgi University, Istanbul, Turkey
61: Also at Rutherford Appleton Laboratory, Didcot, United Kingdom
62: Also at School of Physics and Astronomy, University of Southampton, Southampton, United Kingdom
63: Also at Monash University, Faculty of Science, Clayton, Australia
64: Also at Instituto de Astrofísica de Canarias, La Laguna, Spain
65: Also at Utah Valley University, Orem, USA
66: Also at Beykent University, Istanbul, Turkey
67: Also at Bingol University, Bingol, Turkey
68: Also at Erzincan University, Erzincan, Turkey
69: Also at Sinop University, Sinop, Turkey
70: Also at Mimar Sinan University, Istanbul, Istanbul, Turkey
71: Also at Texas A&M University at Qatar, Doha, Qatar
72: Also at Kyungpook National University, Daegu, Korea